

Deposition of Silver Nanoparticles in Geochemically Heterogeneous Porous
Media: Predicting Particle Mobility From Surface Composition Analysis

by

Shihong Lin

Department of Civil and Environmental Engineering
Duke University

Date: _____

Approved:

Mark R. Wiesner, Supervisor

Heileen Hsu-Kim

P. Lee Ferguson

Thesis submitted in partial fulfillment of
the requirements for the degree of Master of Science in the Department of
Civil and Environmental Engineering in the Graduate School
of Duke University

2011

ABSTRACT

Deposition of Silver Nanoparticles in Geochemically Heterogeneous Porous

Media: Predicting Particle Mobility From Surface Composition Analysis

by

Shihong Lin

Department of Civil and Environmental Engineering
Duke University

Date: _____

Approved:

Mark R. Wiesner, Supervisor

Heileen Hsu-Kim

P. Lee Ferguson

An abstract of a thesis submitted in partial
fulfillment of the requirements for the degree
of Master of Science in the Department of
Civil and Environmental Engineering in the Graduate School
of Duke University

2011

Copyright by
Shihong Lin
2011

Abstract

This study focused on the effect of surface heterogeneity on the affinity of nanoparticle (for that surface) and the viability of using surface composition analysis to facilitate the prediction of such an affinity. The transport of the uncoated silver nanoparticles (AgNPs) in a porous medium composed of silica glass beads partially covered with iron oxide was studied and compared to that in a porous medium composed of unmodified glass beads (GB). It was found that at relative high pH (8.3) there existed only a small difference in AgNPs mobility in both porous media unless the ionic strength was sufficiently high while at lower pH (5) AgNPs had considerably lower affinity for the GB collectors compared to that of the iron oxide coated glass beads (FeO-GB) collectors, even at relative low ionic strengths. There was a linear correlation between the average nanoparticle affinity for media composed of mixtures of FeO-GB and GB collectors and the relative composition of those media as quantified by the mixing mass ratios of the two types of collectors, so that the average AgNPs affinity for these media is readily predicted from the mass (or surface) weighted average of affinities for each of the surface types. Using X-ray Photoelectron Spectroscopy (XPS) to quantify the composition of the collector surface appears to be a viable means to predict the affinity between the nanoparticles and a collector surface with known composition provided that a relevant correlation curve could be established from measured affinity between

the nanoparticles and collector surfaces with similar but different composition (i.e. surfaces with the same components but different proportion of each component).

Contents

Abstract	iv
List of Tables.....	viii
List of Figures.....	ix
1. Introduction and Problem Statement	1
2. Literature Review	5
2.1 Overview of Deposition Study.....	5
2.2 Surface Interaction: the DLVO Theory.....	9
2.2.1 van der Waals Interaction	9
2.2.2 Electrical Double Layer Interaction.....	18
2.2.3 Total Potential Energy for Sphere-Plate Interaction	23
2.2.4 From Energy Curve to Particle Stability	26
2.3 Column Test.....	29
2.3.1 Theory of Transport in Granular Filtration.....	29
2.3.2 Inadequacy of DLVO Theory in Explaining Column Test Data	37
2.4 Deposition onto Heterogeneous Surfaces.....	39
2.4.1 Source and Description of Surface Heterogeneity	39
2.4.2 Particle Deposition onto Heterogeneous Surface.....	41
3. Materials and Methods	44
3.1 Synthesis and Characterization of Silver Nanoparticles	44

3.2 Preparations and Characterizations of Porous Media	46
3.2.1 Preparations of Porous Media.....	46
3.2.2 Characterization of Porous Media	47
3.3 Column Experiment and Determination of Attachment Efficiency	48
3.3.1 Column Experiment	48
3.3.2 Determination of Attachment Efficiency	51
4. Results and Discussion	53
4.1 Properties of Silver Nanoparticles	53
4.2 Morphology and Composition of Collector Surfaces	56
4.3 Surface Chemistry of AgNPs and Collectors	59
4.4 Effect of pH and Ionic Strength on Particle Deposition	60
4.5 Relative Insignificance of Zeta Potential ζ	64
4.6 Correlation between Attachment Efficiency and Surface Composition of Heterogeneous Surfaces	68
5. Conclusion	73
6. Future Work	75
Appendix A: Nomenclatures	77
Appendix B: Abbreviations	81
Reference	82

List of Tables

Table 1: Expression for different types of van der Waals interactions between molecules	11
Table 2: Expressions for non-retarded van der Waals interactions between macroscopic bodies.....	12
Table 3: Summary of existing expressions for potential of EDL interaction for three types of geometries and with three and three type s of interactions.....	21
Table 4: Exact analytical expressions for sphere-plate EDL interaction without using Derjaguin approximation	22
Table 5: Expressions of single collector efficiency contributed by individual mechanisms governing particle transport in a porous medium	33
Table 6: Correlation expressions for single collector efficiency contributed by different mechanisms in granular filtration	34
Table 7: Parameters for Column Experiments.....	50

List of Figures

Figure 1: Representative interaction energy curves based on DLVO theory. The particle size is 100nm (radius) and the surface potential is -25.7mV ($k_B T/e$) for both particle and plate. Hamaker constant is chosen to be 10^{-20} J. The ionic strengths are 0.01M, 0.1M, and 0.5M for the red, blue, and green curves respectively. Born interaction is not considered.	25
Figure 2: Single collector efficiency as a function of particle size under different conditions. (Particle density and Darcy velocity of the carrying flow. Collector diameter is 360 μ m and porosity is 0.4.....	36
Figure 3: Diagram of a column test setup	49
Figure 4: Transmission electron microscopy of charge-stabilized silver nanoparticles (AgNPs).....	54
Figure 5: AgNPs size (diameter) distribution from TEM image analysis	54
Figure 6: UV-Vis spectrum of charge-stabilized AgNPs	55
Figure 7: Scanning electron microscopy image of FeO-GB-HC.....	57
Figure 8: XPS spectra of FeO-GB-HC (top) and FeO-GB-LC (bottom)	58
Figure 9: Zeta potentials of AgNP, GB, and FeO-GB-HC at various pHs (ionic strength was fixed at 0.01 M	60
Figure 10: Representative breakthrough curves for AgNPs deposition in GB (a) and FeO-GB-HC (b) at pH 5	61
Figure 11: Attachment efficiencies between AgNPs and GB (FeO-GB-HC) at various ionic strengths (0.001 M-0.03 M) and pHs (5 and 8.3)	64
Figure 12: Log α_{exp} vs. Φ_{Total} for certain deposition experiments. The α_{exp} is attachment efficiency obtained from column experiments. The energy barrier is calculated using the classic DLVO theory with the measured ζ potentials of the AgNPs and the collectors in the solution chemistry of corresponding experiments. χ is the mass ratio of FeO-GB-HC in a medium composed of a mixture of GB and FeO-GB-HC. All data points were collected with ionic strength fixed at 0.01 M.	66

Figure 13: Attachment efficiencies of AgNPs for bi-component porous media composed of HB and FeO-GB-HC mixed at different ratios and for a mono-component porous medium composed of FeO-GB-LC. All experiments were conducted at an ionic strength of 0.01M and a pH of 5.70

Figure 14: Correlation between the local relative concentrations of Fe and of Ag based on XPS composition analysis. FeO-GB-HC sample collectors were taken carefully from the same longitudinal position in a column that 1 mL of AgNPs passed through.72

Acknowledgements

Thanking someone that I know *I can never thank enough* is sometimes really difficult, especially when you want do it perfect. Nevertheless, I still want to express my deepest gratitude to all those who have been supporting me in so many different ways through these years when I am here at Duke. First of all, I want to thank my advisor, and my mentor, Dr. Mark Wiesner, for his unwavering guidance and support during the past few years of my graduate study. When I applied for graduate school and got accepted by Mark, I was so excited and imaged that I would learn from Mark the “Kung Fu Master” some killer technology or knowledge with which I would also become a “Kung Fu Master” in this field when I graduate. But it is you Mark who let me understand that your role is to direct me to explore independently so that one day I can advance myself to be a “Kung Fu Master”. It is you Mark who inject to us the spirit of exploring and creativity, letting us know that to be a successful graduate student we need to be able to “teach you something” when we graduate. Indeed, while I can always get extremely helpful insights from you when I encounter perplexing problems in research, I can also enjoy the unparalleled academic freedom to explore my own research interest under your direction. I also thank you Mark for being the role model of career passion and work ethic. It is through these years working with you I learn that

any great pursuit, whether academic or others', can be only powered by enthusiasm and accomplished by working hard.

I also thank Dr. Helen Hsu-Kim, Dr. Miguel Medina, Dr. Gabriel Katul, Dr. Claudia Gush, Dr. Andre Khlystov, Dr. Zbigniew Kabala and many more others for their enthusiastic lectures from which I learn a lot, and for their encouragements because of which I desire to learn more. I also owe my gratitude to the members of the Wiesner group—first the “Doctors” including Dr. Benjamin Espinasse, Dr. So-ryong Chae, Dr. Raju Badireddy, Dr. Melanie Auffane, Dr. Jon Brant, Dr. Matt Hotze, Dr. Christine Hendren, Dr. Eric Money, Dr. Esra Erdim, Dr. Hosam Shawky; and then the “to be Doctors” including Jeff Farner, Charles Delanoy, David Jassby, Zach Hendren, Yao Xiao, Mathieu Therezien, Lauren Barton and Liwei Zhang. The group is big, yet you guys make it like a close family. I also thank a colleague and good friend Yingwen Chen from the Chemistry department for his help in many experiments and for his discussion on many ideas.

I want to further thank my committee of Master Thesis including Dr. Mark Wiesner, Dr. Helen Hsu-Kim, and Dr. Lee Ferguson for spending your valuable time and effort in making this possible.

I also thank the lovely and friendly staff in our department, including Dwina Martin, Ruby Nell Carpenter, Rebecca Dupre, Eileen Kramer, Dianne Bennett and others for their scrupulous help on many matters.

There are so many others outside the campus that I am also deeply grateful to, including my dear brothers and sisters in the Duke Chinese Christian Fellowship and Chinese Christian Mission Church. Your friendships, your caring, your encouragements and your prayers are indispensable for me to overcome the hard times in life and to grow in faith.

I also thank my previous and existing roommates Xianrui Cheng, Weiwei Jian, Yi Zhu, Ce Wang, and Wei Kong for caring me like brothers.

Although being on another continent, my parents Shifeng Lin and Xiaoling Lao, and my sister Rushi Lin have never stopped offering me love and caring. Only with their unfaltering love I can feel free to adventure in life knowing that there is always a heartwarming place called home.

1. Introduction and Problem Statement

The recent development of nanotechnology has led to an explosive increase for the production and application of nanomaterials (Wiesner, Lowry et al. 2006; Wiesner and Bottero 2007). Nanomaterials, such as silver nanoparticles (AgNPs), are finding their way into a growing number of commercial products (Creighton, Blatchford et al. 1979; Shiraishi and Toshima 1999; Bosetti, Masse et al. 2002; McFarland and Van Duyne 2003; Baker, Pradhan et al. 2005; Panacek, Kvittek et al. 2006). The broad use of nanomaterials suggests that they will enter into the environment and may pose a threat to human health and the ecosystem (Robichaud, Tanzil et al. 2005; Borm, Robbins et al. 2006; Guzman, Taylor et al. 2006). To assess the environmental implication of existing and emerging nanomaterials, it is essential to understand both the toxicity and the degree of exposure of these materials to human being or other living organisms in interest (Wiesner, Lowry et al. 2006). While recent research has largely focus on the toxicological aspect of nanomaterials, more knowledge about the processes controlling potential exposure to these materials is needed to assess their implications. The degree of exposure of nanomaterials mainly depends on two factors: source quantity and mobility. Aggregation is one of the key processes that controls the mobility of nanoparticles and the aggregation kinetics of various nanomaterials under different environmental conditions have been investigated (Mylon, Chen et al. 2004; Brant, Lecoanet et al. 2005;

Chen and Elimelech 2006; Phenrat, Saleh et al. 2007; Chen and Elimelech 2008; Domingos, Tufenkji et al. 2009; Rebecca and Bojeong 2009). Another key process of determinative effect on the transport of nanomaterials is deposition onto environmental relevant surfaces. Deposition in general refers to the capture of nanoparticles or colloidal particles by surface of collectors of much larger size. These collectors can be immobile such as sands and soils encountered in groundwater aquifers; or they can be mobile such as suspended leaves, silts, fish or even bacteria in the surface water. Aggregation and deposition are similar processes in that they can be both described as the transport of particle, to either collector as in deposition, or to another particle or aggregate of its own kind as in auto-aggregation, followed by the particle-collector or particle-particle attachment the efficiency of which is regulated by surface interaction.

It has become a common routine to quantify the affinity between surfaces using attachment efficiency α which can be defined as the probability of successful attachment per collision between particles or between particle and surface. With known condition of transport, attachment efficiency α can be determined from aggregation or deposition experiments. Many studies focusing on the deposition of nanomaterials have been conducted (Brant, Lecoanet et al. 2005; Espinasse, Hotze et al. 2007; Jaisi, Saleh et al. 2008; Quevedo and Tufenkji 2009). An often-studied surface in deposition experiments is the silica surface, which is considered environmentally relevant. However, most of the

surfaces in the real environment are chemically heterogeneous so that the affinity of nanoparticles for different portions of the surface might be different. It is thus important for us to have a better understanding about how the affinity of nanoparticles for surface is influenced by the mineral heterogeneity of the surface so as to facilitate the assessment of nanoparticle mobility in more complex environments.

In this work, we consider the relative affinity of silver nanoparticles (AgNPs) for two types of surfaces that may be encountered in natural and engineered systems where AgNPs exposure may occur: silica and iron oxide (mainly hematite). The surface charge of these inorganic oxides is strongly dependent on pH. Silica is usually negatively charged over the range of environmental values of pH, while values for the point of zero charge (PZC) for iron oxides are close to the pH of many aquatic environments (Cornell and Schwertmann 1996). This implies that the affinity of negatively charged nanoparticles for an iron oxide surface might be expected to be more sensitive to pH than for a silica surface. Since environmental surfaces are typically heterogeneous, it is important to understand the effect of surface heterogeneity on the affinity of nanoparticles for those heterogeneous surfaces. The goal of the current study is to assess the affinity of AgNPs for a pure silica surface and a heterogeneous surface partially coated with iron oxide and to test the correlation, if there is any, between the affinity of nanoparticle for the collector surface and the surface composition of the collector.

Existing studies used a mixture of negatively charged uncoated quartz sands and positively charged quartz sands that are fully coated with either iron oxyhydroxide (Johnson, Sun et al. 1996) or aminosilane (Abudalo, Bogatsu et al.) and the linear relationship between the attachment efficiency and the ratio of mixing (of the positively charged and negatively charged collectors) was proved with the aminosilane coated collectors. However, it might be questionable that whether such an introduction of the oppositely charged collectors can realistically represent the surface heterogeneity that often occurs locally on a single collector surface. Therefore, it might be helpful to revisit the similar problem using partially modified surface that might mimic the local heterogeneity more realistically. Perhaps more importantly, the heterogeneity parameter χ , which represents the fraction of surface for favorable deposition and was equivalent, in the existing studies, to the proportion of the ideal collector the surface of which was fully coated and positively charged, is hardly a practical parameter for a real environmental surface. It is thus useful to investigate the possibility of employing common surface composition analysis techniques to facilitate the prediction of the affinity of nanoparticles for a heterogeneous surface by using the surface composition as a more pragmatic parameter to describe surface heterogeneity.

2. Literature Review

2.1 Overview of Deposition Study

The study of the deposition of the colloidal particles onto surfaces has attracted extensive attention for the past few decades due to the importance of such a process in numerous fields of science and engineering. Examples include but are not limited to aerosol processing of materials (Gurav, Kudas et al. 1993; Kudas and Hampden-Smith 1999; Chryssolouris, Stavropoulos et al. 2004; Girshick 2008), application of the sol gel process for developing nanostructured thin film on a substrate surface (Hench and West 1990; Lakshmi, Patrissi et al. 1997), the fabrication of novel biomaterials (Bruck 1972; Zhang 2003) and the testing of biocompatibility of these materials. Beyond the applications in material science and biomedical engineering, the particle deposition process also finds paramount importance in many aspects in environmental engineering and science. It is the foundation of several core engineered water treatment processes such as deep bed filtration (Tien and Ramarao 2007) and membrane filtration (Montomery 1985; Mallevalle, Odendaal et al. 1996). It helps us as environmental engineers to better understand processes such as ripening (Clark, Lawler et al. 1992; Moran, Moran et al. 1993) and head-loss buildup (Boller and Kavanaugh 1995; Veerapaneni and Wiesner 1997) in granular filtration, as well as a variety of fouling

processes in different kinds of membrane filtration (Wiesner and Mallevalle 1989; Lahoussine-Turcaud and Wiesner 1990; Lim and Bai 2003). Only with a better knowledge about these processes afforded by advanced understanding in the fundamentals of colloidal deposition can we catch the starting point of improving our existing designs on material, system or operation. Contrary to the processes mentioned above in which the destabilization and removal of the particles is preferred, there are some other engineered processes that entail particle mobility to a certain extent. A typical example would be the recent advancement of using nanoparticles such as nano Zero Valent Iron (nZVI) for ground water remediation (Feitz, Joo et al. 2005; Liu, Majetich et al. 2005; Tratnyek and Johnson 2006; Liu, Phenrat et al. 2007). In this case our knowledge on particle deposition could help us modify the surface the nZVI particles and make them more mobile so that they can be delivered to target contaminated zone (Saleh, Phenrat et al. 2005; Kanel, Choi et al. 2007; Phenrat, Saleh et al. 2008). Beyond the engineering scope, the deposition process is also strongly relevant to environment and human health because it determines the transport and fate of colloids in ground water and other aquatic systems. Among these particles some are by themselves environmental contaminants (Kessler and Hunt ; Buddemeier and Hunt 1988) while some serve as vehicles to facilitate the transport of a variety of other contaminants that otherwise would be relatively immobile without the presence of the colloids (McCarthy and Zachara 1989; Corapcioglu and Jiang 1993; Grolimund, Borkovec et al. 1996; Ryan

and Elimelech 1996). Different types of environmentally relevant particles have been studied, including various minerals, (Marshall and Kitchener 1966; Rajagopalan and Chu 1982; Puls and Powell 1992; Ryde, Kihira et al. 1992) bacteria and viruses, (Logan, Hilbert et al. 1993; Pieper, Ryan et al. 1997; Ryan, Elimelech et al. 1999; Redman, Walker et al. 2004; Walker, Hill et al. 2005) and engineered nanoparticles (Lecoanet, Bottero et al. 2004; Brant, Lecoanet et al. 2005; Saleh, Phenrat et al. 2005; Chen and Elimelech 2006; Espinasse, Hotze et al. 2007; Jaisi, Saleh et al. 2008). The transport and mobility of engineered nanoparticles have been of particular interest over the past few years due to concerns over possible environmental and health impact of these materials (Hoet, Nemmar et al. 1999; Colvin 2003; Borm, Robbins et al. 2006; Renn and Roco 2006; Wiesner, Lowry et al. 2006). As has been pointed out, the potential risk of a certain nanomaterials on human health can be determined by the potential exposure and the toxicity of materials (Robichaud, Tanzil et al. 2005; Wiesner, Lowry et al. 2006), and there is a need to establish a database on the stability and mobility of the interested nanomaterials in relevant environments for the purposes of risk assessment.

Sharing many similarities in nature with particle aggregation, the particle deposition process also has its theoretical foundation that can be dated back to the early study of the stability of lyophobic colloids (Derjaguin and Landau 1941; Verwey and Overbeek 1948) that later become the famous Derjaguin-Landau-Verwey-Overbeek (DLVO) theory named after these four major contributors. Briefly, the DLVO theory

describes the interaction between colloidal particles in a liquid medium by considering the interplay between the ubiquitous van der Waals (vdW) interaction and the electrical double layer (EDL) interaction afforded by the surface charge of the particles (Verwey and Overbeek 1948). By quantifying the interaction using total interaction energy which is the sum of the energy from vdW interaction and the EDL interaction, DLVO theory can be successfully applied to explain and predict the stability of suspension of a variety of lyophobic colloids given the knowledge of solution chemistry and surface chemistry of the particles. Because of the core importance of DLVO theory in understanding the particle deposition process, it is worthwhile for us to review the details of the theory in the following sections.

2.2 Surface Interaction: the DLVO Theory

In this section the Derjaguin-Landau-Verwey-Overbeek (DLVO) theory for modeling the surface interaction (for either particle-particle or particle-collector) is reviewed. It will be shown that under the DLVO theoretical framework, the surface interaction can be viewed as a balance between the two primary interactions: the van der Waals (vdW) interaction and the electrical double layer (EDL) interaction.

2.2.1 van der Waals Interaction

van der Waals forces refer to several categories of interactions that originate from dipole or induced-dipole interactions at the atomic level and yet, can exert observable impact in macroscopic bodies leading to colloidal aggregation (Lyklema, Van Leeuwen et al. 2005) or even the ability of Geckos to walk on walls. Depending on the origin of the interactions, three different types of forces can be classified as the vdW interactions including the London interaction (induced dipole—induced dipole)(London 1930), the Debye interaction (permanent dipole—induced dipole) (Debye 1929) and the Keesom interaction (permanent dipole—permanent dipole)(Keesom 1921) as exemplified by the hydrogen bond. Unlike Keesom and Debye interactions which require the presence of permanent dipole in at least one of the interaction party, the London interaction is always present and thus plays an important role in colloidal and surface phenomena

such as physical adsorption and surface tension (Hunter, White et al. 1987; Hiemenz and Rajagopalan 1997).

The vdW interaction at the molecular level influences the properties and behavior of materials (Hiemenz and Rajagopalan 1997). For example, a gas will condense if the energy of attraction between molecules is large compared to their kinetic energy of the magnitude of $k_B T$. The relative contribution of each force among three types is primarily determined by the dipole moment μ and polarizability α of the interacting molecules. London force would be the major contributor in case of small dipole moment and large polarizability which is exemplified by most of the non-polar organic solvents (Israelachvili 1992). Listed below in Table 1 are the expressions of potential energy of different types of van der Waals interactions between two molecules:

Table 1: Expression for different types of van der Waals interactions between molecules

Type	Nature	Expressions
Debye Interaction	Permanent dipole Vs. Induced dipole	$\Phi_D = -\frac{\alpha_2\mu_1^2 + \alpha_1\mu_2^2}{(4\pi\epsilon_0)^2}x^{-6}$
Keesom Interaction	Permanent dipole Vs. Permanent dipole	$\Phi_K = -\frac{2}{3} \frac{\mu_1^2\mu_2^2}{k_B T (4\pi\epsilon_0)^2} x^{-6}$
London Interaction	Induced dipole Vs. Induced dipole	$\Phi_L = -\frac{hv\alpha_o^2}{2(4\pi\epsilon_0)^2}x^{-6}$ 1 D similar dipoles vibration
		$\Phi_L = -\frac{3hv\alpha_o^2}{4(4\pi\epsilon_0)^2}x^{-6}$ 3 D similar dipoles vibration
		$\Phi_L \approx -\frac{3}{2}h\left(\frac{v_1v_2}{v_1+v_2}\right)\frac{\alpha_{0,1}\alpha_{0,2}}{(4\pi\epsilon_0)^2}x^{-6}$ Dissimilar dipoles vibration

An interesting observation reveals that all these interactions decay as functions of inter-molecular distance to the power of sixth. Thus all these interactions can be grouped into a single expression to describe the net van der Waals interactions using an interaction parameter β^* :

$$\Phi = -\beta^* x^6 \quad \text{Eqn. 1}$$

The van der Waals interaction between two macroscopic bodies that are large compared to the atomic dimension can be evaluated by summing up the pair-wise interactions of constituent molecules in the individual particles (Hamaker 1937). Based on this assumption Hamaker investigated several geometries and gave the expression of non-retarded potential energy for each case. Without diving into the detailed derivation we list some of the expressions on Table 2 (Hiemenz and Rajagopalan 1997).

The Hamaker constant is defined as $A_h = (\rho N_A \pi / M_w)^2 \beta$ and is solely an intensive property of the materials of the interacting objects. The magnitude of the Hamaker ranges from around $4 \times 10^{-20} J$ (e.g. acetone) to around $5 \times 10^{-19} J$ (e.g. gold) (Bargeman and Van Voorst Vader 1972).

Table 2: Expressions for non-retarded van der Waals interactions between macroscopic bodies

Particle Geometry	Expressions
Semi-infinite Half space	$-\frac{A_h}{12\pi d^2}$
Two Spheres	$-\frac{A_h}{6} \left[\frac{2a_{p,1}a_{p,2}}{f(a_{p,1},a_{p,1},d)} + \frac{2a_{p,1}a_{p,2}}{g(a_{p,1},a_{p,1},d)} + \ln \left(\frac{f(a_{p,1},a_{p,1},d)}{g(a_{p,1},a_{p,1},d)} \right) \right]$
Two Plates of Equal Thickness	$-\frac{A_h}{12\pi} \left[\frac{1}{d^2} + \frac{1}{(d+2\delta)^2} - \frac{2}{(d+\delta)^2} \right]$

The above expressions were only for the non-retarded interaction which ignored the effect of time lag on the electromagnetic field by which the London interaction is established. To address this effect we need to consider electromagnetic retardation of the London interaction which accounts for the phase difference that develops between the vibrations at different locations due to the limited speed of light at which the electromagnetic field propagates (Casimir and Polder 1946). Such an effect becomes noticeable as the interacting distance becomes comparable to the wavelength of the propagating field. The detailed analysis of this retardation effect is beyond the scope of this thesis. For practical purpose, Gregory derived approximations for the retarded van der Waals interactions between plates, between spheres and for the sphere-plate system (Gregory 1981). For the study of particle deposition onto a collector that is significantly larger compared to the particles, the sphere-plate approximation is often used:

$$V_{vdW,sp} = -\frac{A_h a_p}{6d} \left(\frac{1}{1+14d/\lambda} \right) \quad \text{Eqn. 2}$$

where A_h is the Hamaker constant of the system, a_p is the radius of the sphere, d is the separation distance (the smallest distance between the surface of the sphere and the plate), λ is the “characteristic wavelength” of the interaction which often assumed to be about 100nm. Other expressions regarding the retarded van der Waals interactions for sphere-sphere or sphere-plate geometries can also be found in literatures. (Schenkel and

Kitchener 1960; Ho and Higuchi 1968; Czarnecki and Itschenskij 1984; Elimelech, Williams et al. 1998).

Not mentioned in the above discussion is the effect of the medium in which the interacting particles are dispersed; or the effect of dissimilarity--if the interacting bodies are of different materials. Fortunately, there is a relatively simple solution to account for these effects due to the convenient fact that the potential energy is always a product of two terms independent of each other: a geometry term, which is solely determined by the shape of the interacting bodies, and the Hamaker constant, which is characteristic of the materials. Thus it becomes possible to account for the effect of the dispersion medium as well as the difference in materials of the interacting bodies by just modifying the Hamaker constant of the system. (Gregory 1970; Bargeman and Van Voorst Vader 1972; Hiemenz and Rajagopalan 1997; Lyklema, Van Leeuwen et al. 2005).

For the case in which two identical particles of Hamaker constant A_{22} are interacting through vdW force in a medium of Hamaker constant A_{11} , the Hamaker constant between the particles in the dispersion medium can be written in as:

$$A_{121} = A_{11} + A_{22} - 2A_{12} \quad \text{Eqn. 3}$$

If we approximate A_{12} using $\sqrt{A_{11}A_{22}}$, Eqn. 3 simplifies to:

$$A_{121} = (A_{22}^{1/2} - A_{11}^{1/2})^2 \quad \text{Eqn. 4}$$

With such an approximation, the effective Hamaker constant for the interaction between particles (of the same kind) in a medium can be conveniently expressed as a function of the Hamaker constants (as in vacuum) of the particles and that of the dispersion medium. There are several implications of this expression worth further discussion. First, the non-negative value of this effective Hamaker constant indicates that the vdW interaction would be always attractive between identical particles (as in homogeneous aggregation) independent of the medium in which the particles are dispersed, except for a very rare case where $A_{11} = A_{22}$ and the particles would not be able to feel a net van der Waal interaction. This rare exception of nature can in fact be scrupulously employed to create certain desirable experimental condition. For example, the Hamaker constant of the liquid phase can be estimated in a semi-classical approach using its surface tension which is readily measurable by other experimental methods. By varying the composition of a liquid mixture in the dispersion medium until attraction between identical particles embedded in that medium disappears, it is feasible to estimate the Hamaker constant of the particles using the Hamaker constant of the liquid mixture calculated from the surface tension. Another application is to eliminate the effective vdW interaction between the particles by again varying the composition of the dispersion medium so as to produce a more controlled condition and facilitate the experimental study of electrostatic interactions. Due to the fact that the Hamaker constants of particles in solid phases are usually higher than that of their liquid phase dispersion medium, another

important implication of the above expression would be that the vdW interactions between identical particles would be weakened by the dispersion medium. Such an effect would be more salient for particles with low Hamaker constants such as polystyrene. For example, the Hamaker constant for polystyrene is $A_{22} \sim 8 \times 10^{-20} J$ and the Hamaker constant for water is $A_{11} \sim 4.35 \times 10^{-20} J$. A simple calculation based on the above expression would give an effective Hamaker constant of around $0.55 \times 10^{-20} J$ for the van der Waals attraction between polystyrene particles dispersed in water—less than one tenth of its counterpart in vacuum. The practical range for Hamaker constants in aqueous dispersion lies between $0.3 - 10 \times 10^{-20} J$ (Elimelech, Williams et al. 1998) with dense particles having values towards the upper end of the range while low-density particle (e.g. biological materials) approaching the lower limit.

The effective Hamaker constant for the vdW interaction between particles of different materials dispersed in a medium can be reached in the same approach as that for identical particles. Using the same notations as the above discussion but now for the particle of different material let it be assigned a Hamaker constant of A_{33} , the effective Hamaker constant for the interaction between particle 2 and 3 that are dispersed in medium 1 would be:

$$A_{312} = A_{11} + A_{23} - A_{12} - A_{13} \quad \text{Eqn. 5}$$

Applying again the approximation that $A_{ij} = \sqrt{A_{ii}A_{jj}}$ leads to a factored expression:

$$A_{312} = (A_{33}^{1/2} - A_{11}^{1/2})(A_{22}^{1/2} - A_{11}^{1/2}) \quad \text{Eqn. 6}$$

This is a useful expression to evaluate the vdW interaction in heterogeneous aggregation or deposition of colloid particles. In the later part of this thesis the deposition of silver nanoparticles onto silica surface is investigated. The Hamaker constant for amorphous silica is about $6.5 \times 10^{-20} J$ (Bergstrom 1997) while that for silver is about $40 \times 10^{-20} J$ (Bargeman and Van Voorst Vader 1972). Thus the calculated effective Hamaker constant $A_{Ag-W-Si}$ is $1.97 \times 10^{-20} J$.

Unlike the vdW interaction between two identical particles, which is always attractive, vdW can be repulsive as the Hamaker constant for interaction between dissimilar objects in a medium can become negative. The only requirement to meet to generate such a situation is that the Hamaker constant of the medium falls between Hamaker constants of the interacting materials. A perfect example would be the repulsive van der Waals force between most of the colloidal particles and the water/air interface. Again taking silver nanoparticles as an example and assuming that the Hamaker constant for air is close to that of vacuum which is 0, the calculated effective Hamaker constant $A_{Ag-W-Air}$ would be around $-8.8 \times 10^{-20} J$ --implying that the vdW interactions is repulsive for the Ag nanoparticles at the air-water-interface (AWI).

2.2.2 Electrical Double Layer Interaction

Particles usually bare charges on their surfaces by one or more of several possible mechanisms (The first common mechanism is the preferential adsorption of ions from the solution where the particles are suspended. A classic example of this is the silver iodide (AgI) sol which was extensively used as the model colloid during the time when the DLVO theory was being established. (Verwey 1935). In the dispersing solution with excess amount of Ag^+ or I^- , the surface of the AgI nanoparticles is charged and the electrostatic repulsion between the charged surfaces stabilizes the particle suspension. Another commonly encountered mechanism is the ionization or dissociation of a surface group such as a carboxyl group or a hydroxyl group. As an example, many metal oxides establish their surface charge by protonation or de-protonation of the $\equiv \text{MeOH}$ surface group(Stumm, Sigg et al. 1992). For the case of clay minerals, an important mechanism is that of crystal lattice defects (also called isomorphous substitution) with which certain native elements of compounds are substituted by some alien elements without the alternation of the lattice structure (Hunter, White et al. 1987; Lyklema, Van Leeuwen et al. 2005). The particles will be charged if the substituting ions and the substituted ions are of different valences.

When the charged particles are submerged in solution of ions (either common ions or indifferent ions), the distribution of the ions in the solution will be affected by the electrical field that emanates from the charged surface of particles. The distribution of

this ionic cloud can be theoretically described by the Poisson-Boltzmann equation which states that:

$$\nabla^2 \psi = -\frac{\rho^*}{\epsilon_0 \epsilon_r} = -\frac{1}{\epsilon_0 \epsilon_r} \sum z_i e n_{i,\infty} \exp\left(\frac{-z_i e \psi}{k_B T}\right) \quad \text{Eqn. 7}$$

When the surface potential is low such that the electrical energy is small compared to the thermal energy ($|ze\psi| \ll k_B T$), the Debye-Huckel approximation can be applied, leading to the linearized Poisson-Boltzmann equation:

$$\nabla^2 \psi = \left(\frac{\sum z_i^2 e^2 n_i^0}{\epsilon k_B T} \right) \psi = \kappa^2 \psi \quad \text{Eqn. 8}$$

where κ is called the Debye constant and $1/\kappa$ is named as the Debye length and widely adopted as the extension (or thickness) of the double layer. For a planar geometry, the linearized Poisson-Boltzmann equation has a simple solution as $\psi = \psi_o \exp(-\kappa x)$; for a spherical geometry the solution would be $\psi = \psi_o a_p \exp[-\kappa(r - a_p)]/r$. There are other simplified solutions for different geometries when the condition $|ze\psi| \ll k_B T$ is not satisfied, such as the Gouy-Chapman solution for details (Verwey and Overbeek 1948).

Although the double layer theory is the foundation and starting point to understand the electrostatic interaction between charged surfaces, what really interests us eventually is the potential energy associated with the electrostatic interaction, or more precisely, the overlapping of the double layers, which can be used to compared

with the potential energy of vdW interaction to give a full picture of interaction between particles. Detailed treatments about this subject can be found in numerous classic text and literatures (Derjaguin 1940; Verwey and Overbeek 1948; Hunter, White et al. 1987; Hiemenz and Rajagopalan 1997; Lyklema, Van Leeuwen et al. 2005). Shown on Table 3 are the most commonly used expressions of potential of EDL interaction for plate-plate, sphere-sphere, and sphere-plate system based on constant potentials (CP), constant charge (CC), and linear superposition approximation (LSA) assumptions (Hogg, Healy et al. 1966; Wiese and Healy 1970; Gregory 1975). Among equations based on three different assumptions, the LSA-based expression was considered as the one that would give an intermediate value that is closest to the realistic scenario (The sphere-sphere and sphere-plate expressions are based on Derjaguin approximations and they are thus only applicable for interaction of “thin double layer” (as compared to the particle size, i.e. $\kappa_p \gg 1$) (For the case of sphere-plate interaction only, Lin and Wiesner proposed a set of expressions for the potential of EDL interaction obtained without resorting to the Derjaguin approximation (Lin and Wiesner 2010) and they are listed on Table 4.

Table 3: Summary of existing expressions for potential of EDL interaction for three types of geometries and with three and three type s of interactions

Geometry	Type	Expressions	Eqn.
	CP	$V_{PP}^{\psi} = \frac{\epsilon\kappa}{2} [(\psi_{p1}^2 + \psi_{p2}^2)(1 - \text{Coth}(\kappa L)) + 2\psi_{p1}\psi_{p2}\text{Csch}(\kappa L)]$	Eqn.9
Plate Plate $V_{PP}(L)$	CC (Linearized PB)	$V_{PP}^{\psi} = \frac{\epsilon\kappa}{2} [(\psi_{p1}^2 + \psi_{p2}^2)(\text{Coth}(\kappa L) - 1) + 2\psi_{p1}\psi_{p2}\text{Csch}(\kappa L)]$	Eqn.10
	CC (Compression)	$V_{PP,compression}^{\sigma} = \epsilon\kappa \left(\frac{k_B T}{ze}\right)^2 \left[2\bar{y} \ln\left(\frac{B + \bar{y} \coth(kL/2)}{1 + \bar{y}}\right)\right]$	Eqn. 11
	LSA	$V_{PP}^{LSA} = 32\epsilon\kappa \left(\frac{k_B T}{ze}\right)^2 \gamma_{p1}\gamma_{p2} \exp(-\kappa L)$	Eqn. 12
Sphere Sphere $V_{SS}(d)$	CP (Linearized PB)	$V_{SS}^{\psi} = \frac{\pi\epsilon a_1 a_2}{a_1 + a_2} \left[(\psi_{s1}^2 + \psi_{s2}^2) \ln(1 - e^{-2\kappa d}) + 2\psi_{s1}\psi_{s2} \ln\left(\frac{1 + e^{-\kappa d}}{1 - e^{-\kappa d}}\right) \right]$	Eqn. 13
	CC (Linearized PB)	$V_{SS}^{\psi} = \frac{\pi\epsilon a_1 a_2}{a_1 + a_2} \left[-(\psi_{s1}^2 + \psi_{s2}^2) \ln(1 - e^{-2\kappa d}) + 2\psi_{s1}\psi_{s2} \ln\left(\frac{1 + e^{-\kappa d}}{1 - e^{-\kappa d}}\right) \right]$	Eqn. 14
	LSA	$V_{SS}^{LSA} = 64\pi\epsilon \frac{a_1 a_2}{a_1 + a_2} \left(\frac{k_B T}{ze}\right)^2 \gamma_{s1}\gamma_{s2} \exp(-\kappa d)$	Eqn. 15
Sphere Plate $V_{SP}(H_0)$	CP (Linearized PB)	$V_{SP}^{\psi} = \pi\epsilon a \left[(\psi_s^2 + \psi_p^2) \ln(1 - e^{-2\kappa H_0}) + 2\psi_s\psi_p \ln\left(\frac{1 + e^{-\kappa H_0}}{1 - e^{-\kappa H_0}}\right) \right]$	Eqn. 16
	CC (Linearized PB)	$V_{SP}^{\sigma} = \pi\epsilon a \left[-(\psi_s^2 + \psi_p^2) \ln(1 - e^{-2\kappa H_0}) + 2\psi_s\psi_p \ln\left(\frac{1 + e^{-\kappa H_0}}{1 - e^{-\kappa H_0}}\right) \right]$	Eqn. 17*
	LSA	$V_{SP}^{LSA} = 64\pi\epsilon a \left(\frac{k_B T}{ze}\right)^2 \gamma_p\gamma_s \exp(-\kappa H_0)$	Eqn. 18*
Definitions		$\gamma_x = \tanh\left(\frac{y_x}{4}\right)$ Eqn. 19	$y_x = \frac{ze\psi_x}{k_B T}$ Eqn. 20
		$B = [1 + \bar{y} \csc^2(\kappa d / 2)]^{1/2}$ Eqn. 21	$\bar{y} = \frac{1}{2}(y_{p1} + y_{p2})$ Eqn. 22

* The original publications did not present the expressions for the sphere-plate geometry, but it takes a minimal modification to arrive at these expression from their sphere-sphere counterparts.

Table 4: Exact analytical expressions for sphere-plate EDL interaction without using Derjaguin approximation

Type	Expression	Equation
CP	$V_{SP^*}^\psi = [V_{SP}^\psi(H_0) + V_{SP}^\psi(H_0 + 2a)] + [\beta^\psi(H_0) - \beta^\psi(H_0 + 2a)]$	Eqn. 23
	$\beta^\psi(x) = \frac{\pi\epsilon}{\kappa} \left[\frac{1}{2}(\psi_{sph}^2 + \psi_{pl}^2) Li_2(e^{-2\kappa x}) + 2\psi_{sph}\psi_{pl} [Li_2(-e^{-\kappa x}) - Li_2(e^{-\kappa x})] \right]$	Eqn. 24
LSA	$V_{SP^*}^{LSA} = V_{SP}^{LSA}(H_0) + V_{SP}^{LSA}(H_0 + 2a) + \frac{64\pi\epsilon}{\kappa} \left(\frac{k_B T}{ze} \right)^2 \gamma_{sph}\gamma_{pl} [-e^{-\kappa H_0} + e^{-\kappa(H_0 + 2a)}]$	Eqn. 25
CC	$V_{SP^*}^\sigma = [V_{SP}^\sigma(H_0) + V_{SP}^\sigma(H_0 + 2a)] + [\beta^\sigma(H_0) - \beta^\sigma(H_0 + 2a)]$	Eqn. 26
(LPB based)	$\beta^\sigma(x) = \frac{\pi\epsilon}{\kappa} \left[-\frac{1}{2}(\psi_{sph}^2 + \psi_{pl}^2) Li_2(e^{-2\kappa x}) + 2\psi_{sph}\psi_{pl} [Li_2(-e^{-\kappa x}) - Li_2(e^{-\kappa x})] \right]$	Eqn. 27

V_{SP}^ψ , V_{SP}^σ , and V_{SP}^{LSA} are the existing expressions for potential energy of EDL interaction for a sphere-plate system as modified from those for sphere-sphere interaction obtained using the Derjaguin Approximation. They are listed on Table 3 as eqn.16, eqn. 17, and eqn. 18 respectively.

2.2.3 Total Potential Energy for Sphere-Plate Interaction

Now with a brief review of the van der Waals interaction and the electrostatic interaction, the building blocks have been collected to construct the DLVO theory for describing the colloidal stability, or in our context, the affinity between a particle and a relative large collector that can be modeled as a semi-infinite body. Considering only the two essential types of interactions discussed above, the total interaction between a sphere and a collector as expressed in total potential energy V_{Tot} , is the sum of the van der Waals interaction V_{vdW} and the electrostatic interaction V_{EDL} .

$$V_{Tot} = V_{vdW} + V_{EDL} \quad \text{Eqn. 28}$$

There is one more interaction that always exists but only becomes prominent when the interacting surfaces are close enough to each other. It is called the Born repulsion--a short-range interaction stemming from the strong repulsive forces between atoms as their electron clouds start to overlap. A practical approximation was given by Ruckenstein and Prieve (Ruckenstein and Prieve 1976):

$$V_{Born} = \frac{A\sigma_c^6}{7560} \left[\frac{8a_p + d}{(2a_p + d)^7} + \frac{6a_p - d}{d^7} \right] \quad \text{Eqn. 29}$$

where σ_c is the called the collision diameter and typically of the order of 0.5nm.

With the short range Born repulsion being considered, the total interaction potential energy then becomes $V_{Tot} = V_{vdW} + V_{EDL} + V_{Born}$ (Eqn. 30). Depending on the interacting system, there may also exist some other forces that are not of DLVO nature such as structural force, hydration force, hydrophobic force, and steric force as for coated particles. Systematic review of these forces can be found in literature or textbook. (Israelachvili 1992; Grasso*, Subramaniam et al. 2002)

Similar to all of its components, V_{Tot} is a function of the separation distance. By plotting V_{Tot} against the separation distance, an energy curve can be obtained to describe the stability of the interacting system. As can be observed from the equations, the van der Waals interaction is characteristic of the material and geometry of the interacting objects and does not change with the solution chemistry. (Although some argues that vdW interaction can also occurs through the dispersion force between the particle and the electrolyte in the medium(Grasso*, Subramaniam et al. 2002).) Therefore, for a given system, the shape of the energy curve is usually determined by two variable factors: surface potential ψ_0 which is affected by pH or common ions whenever they are present and relevant, and ionic strength I which would affect the Debye constant κ of the electrical double layer and thus the potential energy for electrostatic interaction.

There are three different possibilities for the shapes of the total potential energy curves. Because force is the spatial derivative of potential energy, the stability of the system associated with a specific type of energy curve can be determined. Three

different types of interaction curves were generated by varying the surface potential and the ionic strength and they are presented on Figure 2.

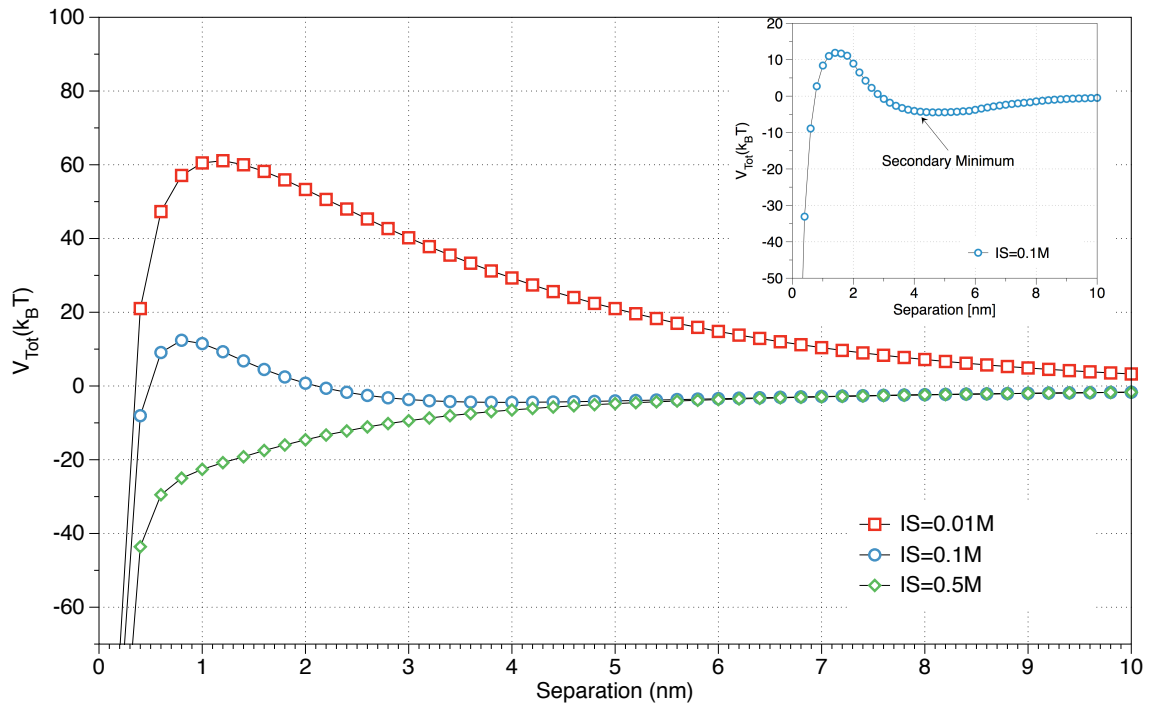


Figure 1: Representative interaction energy curves based on DLVO theory. The particle size is 100nm (radius) and the surface potential is $-25.7mV$ ($k_B T/e$) for both particle and plate. Hamaker constant is chosen to be $10^{-20}J$. The ionic strengths are 0.01M, 0.1M, and 0.5M for the red, blue, and green curves respectively. Born interaction is not considered.

It is worth noting that one type of energy curve involves an energy barrier as well as a secondary minimum (the curve with circles in Figure 1) that may be responsible for a metastable condition. This type of energy curve is often a consequence of both relatively high surface potential and relatively high ionic strength. For a given system (i.e. given Hamaker constant and particle size) there exists a relative small “window” of surface potentials and pH in which a significantly deep secondary

minimum can occur. While particle deposition into the primary minimum is usually considered irreversible, particle deposition into the secondary minimum is however reversible if a later change of solution chemistry would result in the first type of energy curve (the curve with squares in Figure 1). This phenomenon has actually been observed in experiments. (Litton and Olson 1996; Tufenkji and Elimelech 1999; Hahn, Abadzic et al. 2004; Renn and Roco 2006)

2.2.4 From Energy Curve to Particle Stability

To quantify the stability of particles in the context of the deposition, it would be convenient to use the concept of attachment efficiency α which is defined as the probability of successful attachment between the particles and the collector surface per collision. It is in fact the reciprocal of a long established concept--stability ratio W . (Fuchs 1934; Verwey and Overbeek 1948). For interaction between spherical particles, Fuchs derived an expression of W based on the O_{ut} when only the vdW and EDL interactions were considered:

$$W = 2 \int_0^{\infty} \frac{e^{V_{Tot}/k_B T}}{(u+2)} du \quad \text{Eqn. 31}$$

Where $u = H_0 / 2(a_{p,1} + a_{p,2})$. For sphere-plane interactions as encountered in the context of particle deposition in unfavorable conditions, α can also be viewed as the ratio of the single-collector efficiency (η , which is defined in the next section) with the both the vdW attraction and EDL repulsion to that when only vdW interaction remains (η_0). In other

words, the attachment coefficient presents the ratio of contacts that particles make with a collector surface that result in attachment to the total number of contacts. While it is often assumed that α is a function of the conditions of surface chemistry alone, a more exact relationship between the α and the V_{Tot} for transport in a porous medium includes hydrodynamic effects on α . An approximate expression was given by Spielman and Friedlander (Spielman and Friedlander 1974):

$$\alpha = \left(\frac{\beta}{1 + \beta} \right) S(\beta) \quad \text{Eqn. 32}$$

where $S(\beta)$ is a function of β with tabulated values given by Spielman and Friedlander and β is defined as:

$$\beta = \frac{1}{3} 2^{1/3} \Gamma(1/3) A_s^{-1/3} \left(\frac{D_\infty}{U a_c} \right)^{1/3} \left(\frac{K_F a_c}{D_\infty} \right) \quad \text{Eqn. 33}$$

K_F is the pseudo-first-order rate constant given by:

$$K_F = \frac{D_\infty}{\int_0^\infty [f(h, a_p) e^{V_{\text{Tot}}/k_B T} - 1] dh} \quad \text{Eqn. 34}$$

$f(h, a_p)$ is a function that accounts for the reduced mobility due to hydrodynamic interactions when the particles are close to the surface. Dahneke (Dahneke 1974) suggested a simple approximation for this function:

$$f(h, a_p) = 1 + a_p / h \quad \text{Eqn. 35}$$

Calculations based on the above expressions yield the theoretical value of α as a function of surface potentials, ionic strength, Hamaker constant and particle sizes. The theoretical relationships between the predicted α and these parameters have been studied and illustrative examples were given (Several general trends can be observed: (1) α increases with increasing ionic strength until the ionic strength reaches a certain level which is termed as the critical deposition concentration (CDC). At CDC the deposition process transits from the unfavorable deposition to the favorable deposition. Before CDC is reached, the slope describing the increase of $\log \alpha$ as a function of $\log IS$ is steeper for larger particle size. (2) α decreases with increasing surface potentials (of either ψ_p or ψ_c). The slope describing the decrease $\log \alpha$ as $\log \psi$ increases is independent of the ionic strength but becomes steeper again for larger particle size; (3). Increasing the Hamaker constant decreases the CDC. But the slope describing the increase of $\log \alpha$ as a function of $\log IS$ is independent of the Hamaker constant. (Elimelech and Omelia 1990)

2.3 Column Test

2.3.1 Theory of Transport in Granular Filtration

One of the most widely used experimental techniques to evaluate α is column test which has its origin in the study of water and wastewater filtration. (Yao, Habibian et al. 1971) Briefly, a column test is an experiment to assess the affinity between the particle and the collector surface by measuring the removal efficiency of the particles in a controlled flow through a porous medium composed of collectors that are ideally of known geometry which can be accounted for in transport equations. The removal of particles from a suspension involves two processes--the transport of particles to the vicinity of collector surface and the ensuing attachment (Ives and Gregory 1966; O'Melia and Stumm 1967). The governing equation to describe the concentration distribution for Brownian particles in the presence of particle-collector interaction can be written as (Spielman and Fitzpatrick 1973; Tien and Ramarao 2007):

$$\frac{\partial C}{\partial t} + \vec{v} \cdot \nabla C = \nabla \cdot (D \nabla C + m C \nabla V_{Tot}) \quad \text{Eqn. 36}$$

where C is the number concentration of the particle, v is the flow velocity, D is the diffusion coefficient, m is the particle mobility and V_{Tot} the total interaction potential energy. For a packed column, it is helpful to introduce the single collector efficiency (η)

which is defined as the ratio of the rate at which the particles strike the collector to the rate at which the particles approach the projected area of the collector from the upstream (Yao, Habibian et al. 1971). Based on mass balance, and ignoring diffusion or dispersion in the column, the change in particle concentration along the direction of macroscopic flow in a column of porosity ε can be described as:

$$\frac{dC}{dx} = -\frac{3}{2} \frac{1-\varepsilon}{d_c} \alpha \eta C \quad \text{Eqn. 37}$$

where d_c is the diameter of the collectors that constitute the column. Integration of the above equation leads to:

$$\ln\left(\frac{C_{eff}}{C_{inf}}\right) = -\frac{3}{2}(1-\varepsilon)\eta \frac{L}{d_c} = -\frac{3}{2}(1-\varepsilon)\alpha\eta_0 \frac{L}{d_c} \quad \text{Eqn. 38}$$

where C_{eff} is the particle concentration at the effluent and C_{inf} the particle concentration at the influent. Rearranging the above equation gives:

$$\alpha = -\frac{1}{\eta_0} \frac{2d_c}{3(1-\varepsilon)L} \ln \frac{C_{eff}}{C_{inf}} \quad \text{Eqn. 39}$$

The above equation allows for the attachment efficiency α to be calculated from the physical transport of particles through the column as expressed by the calculated η_0 , and

from the measurable removal efficiency of particles across the column as expressed by $C_{\text{eff}}/C_{\text{inf}}$. While d , ε and L are characteristic parameters of the column and the collectors and thus readily accessible, $L\ln(C_{\text{eff}}/C_{\text{inf}})$ is measured by experiments. The single collector efficiency η_0 must be calculated from theory.

There are usually two approaches to obtaining estimates of the attachment efficiency. The first one takes advantage of the definition that $\alpha=\eta/\eta_0$. Assuming in favorable conditions that $\eta=\eta_0$ ($\alpha=1$), it is possible to adjust the solution chemistry such that the EDL interaction between the particles and the collector surface become attractive. One possible way is to adjust the pH of the background solution such that the signs of charges on the collector surface and on the particles become opposite. Another way is to modify the surface of the collector by certain coatings (e.g. aminosilane) to make it positively charged when the particles are negatively charged (Redman, Walker et al. 2004). Under such a favorable deposition condition:

$$\ln\left(\frac{C_{\text{eff},\text{fav}}}{C_{\text{inf}}}\right) = -\frac{3}{2}(1-\varepsilon)\eta_0 \frac{L}{d_c} \quad \text{Eqn. 40}$$

For the unfavorable deposition with other experimental parameters unchanged:

$$\ln\left(\frac{C_{eff,unfav}}{C_{inf}}\right) = -\frac{3}{2}(1-\varepsilon)\eta\frac{L}{d_c} \quad \text{Eqn. 41}$$

Combining the above two equation would give:

$$\alpha = \frac{\eta}{\eta_0} = \ln\frac{C_{eff,unf}}{C_{eff,fav}} \quad \text{Eqn. 42}$$

The second approach requires the estimation of the η_0 based using a correlation equation based on other parameters. One of the early attempts to assess η_0 was given by Yao and O'Melia (Yao and O'Melia 1968) who solved the convective-diffusion transport equation numerically. It was also pointed out that η is composed of three different component based on transport mechanisms, each of which can be expressed analytically assuming that only one of its corresponding transport mechanism is operative (Yao, Habibian et al. 1971).

$$\eta = \eta_D + \eta_I + \eta_G \quad \text{Eqn. 43}$$

Listed in Table 5 are these mechanisms and their corresponding analytical expressions to illustrate the governing parameters in each mechanism:

Table 5: Expressions of single collector efficiency contributed by individual mechanisms governing particle transport in a porous medium

Mechanism	Analytical Expression	Equation	Reference
Brownian Diffusion	$\eta_D = 4.04Pe^{-2/3} = 0.9 \left(\frac{k_B T}{\mu d_p d_c U} \right)^{2/3}$	Eqn. 44	(Levich 1962)
Interception	$\eta_I = \frac{3}{2} \left(\frac{d_p}{d_c} \right)^2$	Eqn. 45	(Yao, Habibian et al. 1971)
Gravitational Sedimentation	$\eta_G = \frac{(\rho_p - \rho_w)}{18\mu U} g d_p^2$	Eqn. 46	(Yao, Habibian et al. 1971)

Although numerical solution of convective-diffusion describes the transport process in a comparatively accurate manner, a closed form solution is of greater practical use. Rajagopalan and Tien (Rajagopalan and Tien 1976) proposed a semi-empirical correlation equation (RT correlation) based on the trajectory analysis of the filtration with the sphere-in-cell porous media model. The RT correlation has been widely applied to predict the particle deposition process in various systems (Martin, Bouwer et al. 1992; Hsu, Huang et al. 2001). Tufenkji and Elimelech (Tufenkji and Elimelech 2004) later suggested what they considered to be an improved version of the correlation equation (TE correlation) in which the hydrodynamic and the van der Waals interactions were incorporated. The TE correlation was shown to be in a better agreement with the

numerical solution of the transport equation over the range of conditions used to develop the correlation.

Table 6: Correlation expressions for single collector efficiency contributed by different mechanisms in granular filtration

Mechanism	Correlation Expression	Equation
Brownian diffusion	$\eta_D = 2.4 A_S^{1/3} N_R^{-0.081} N_{Pe}^{-0.715} N_{vdW}^{0.052}$	Eqn. 47
Interception	$\eta_I = 0.55 A_S N_R^{1.675} N_A^{0.125}$	Eqn. 48
Gravitational Sedimentation	$\eta_G = 0.475 N_R^{-1.35} N_{Pe}^{-1.11} N_{vdW}^{0.053} N_{gr}^{1.11}$	Eqn. 49
Parameter	Definition	Physical interpretation
N_R	d_p / d_c	Aspect ratio
N_{Pe}	$U d_c / D_\infty$	Peclet number characterizing ratio of convective transport to diffusive transport
N_{vdW}	$A_h / k_B T$	van der Waals number characterizing ratio of van der Waals interaction energy to the particle's thermal energy
N_{gr}	$\frac{4 \pi a_p^4 (\rho_p - \rho_w) g}{3 k_B T}$	Gravitational number: ratio of particle's gravitational potential when located one particle radius from collector to particle's thermal energy
N_A	$\frac{A}{12 \pi \mu a_p^2 U}$	Attraction number: represents combined influence of van der Waals attraction forces and fluid velocity on particle deposition rate due to interception

Table 6: Correlation expressions for single collector efficiency contributed by different mechanisms in granular filtration (Continued)

N _G	$\frac{2 a_p^2 (\rho_p - \rho_w) g}{9 \mu U}$	Gravity number: ratio of Stokes particle settling velocity to approach velocity of the fluid
----------------	---	--

*Modified from Tufenkji and Elimelech(Tufenkji and Elimelech 2004).

There exists a size of particle (on the order of 1µm for typical condition of water filtration) for which the removal efficiency reaches the minimum (Yao, Habibian et al. 1971). Because the mechanism for the removal of smaller particles is dominated by Brownian diffusion and that for the removal of larger particles is controlled by interception and sedimentation, η takes on larger values at both ends of the particle size spectrum. Figure 2 is a demonstration of this effect using the TE correlation and a set of arbitrary parameters.

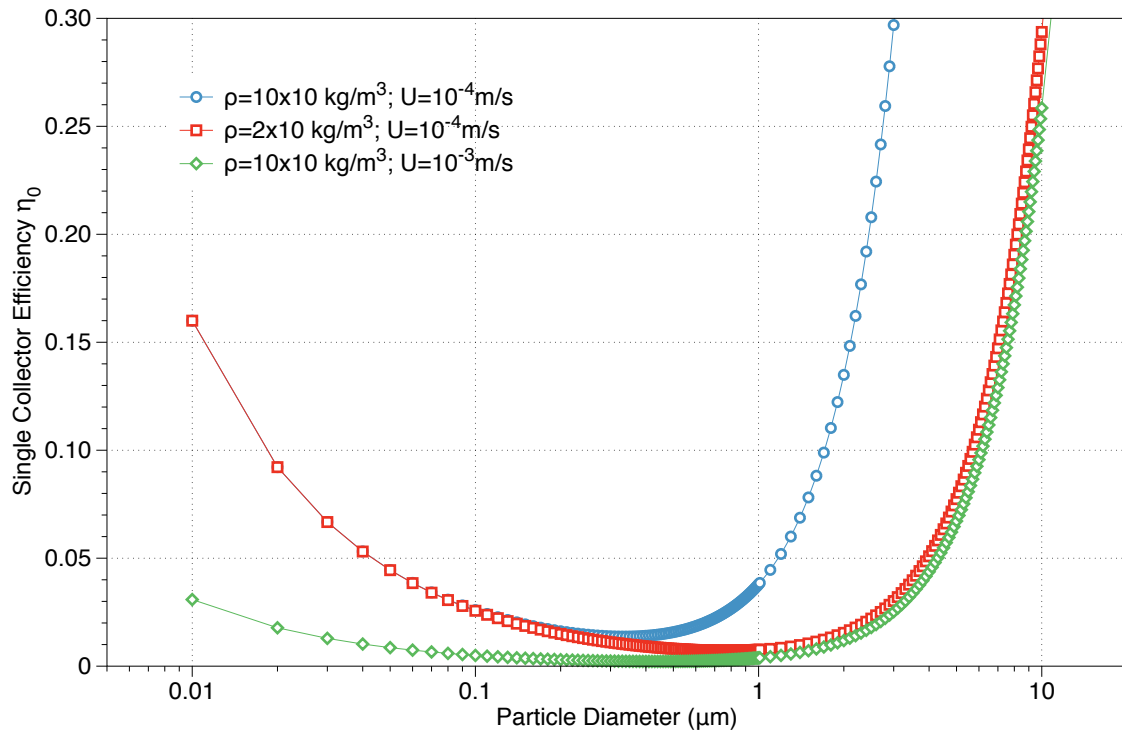


Figure 2: Single collector efficiency as a function of particle size under different conditions. (Particle density and Darcy velocity of the carrying flow. Collector diameter is 360 μm and porosity is 0.4.

2.3.2 Inadequacy of DLVO Theory in Explaining Column Test Data

The employment of DLVO theory to describe the kinetics of particle deposition was successful in qualitatively explaining many experimental results. However, several important deviations of experimental data from the numerical results based on DLVO theory were also observed (Gregory and Wishart 1980; Yoshimura 1980; Tobiasson and O'melia 1988; Elimelech and Omelia 1990; Vaidyanathan and Tien 1991; Litton and Olson 1993). For example, it was found that the change of α with respect to the change of ionic strength is far less sensitive than theoretical prediction. While the observed CDC was close to that from theoretical prediction, the observed α was orders of magnitude higher than the predicted value when the IS is below CDC. In addition, DLVO theory predicts that the shape of the $\log\alpha$ - $\log C_s$ curve should be sensitive to the size of particle. Smaller particles should theoretically have a higher CDC and a higher sensitivity of α to the change of C_s when C_s is below the CDC. However, little difference is observed experimentally between the $\log\alpha$ - $\log C_s$ curves of large and small particles. Several possible explanations were proposed for these disparities as well as the similar disparities observed in the kinetics of aggregation, including distribution of surface properties (Prieve and Ruckenstein 1980; Tobiasson 1987; Elimelech and Omelia 1990; Vaidyanathan and Tien 1991), surface charge heterogeneity (Hull and Kitchener 1969; Bowen and Epstein 1979; Gregory and Wishart 1980; Adamczyk 1983; Sjollema, Busscher et al. 1989; Busscher, Sjollema et al. 1990; Vaidyanathan and Tien 1991; Kihira and

Matijevic 1992), surface roughness of particles and collectors (Reerink and Overbeek 1954; Marshall and Kitchener 1966; Hull and Kitchener 1969; Overbeek 1982; Czarnecki 1986), dynamics of interaction (Leeuwen and Lyklema ; Dukhin and Lyklema 1987), deposition into secondary minima (Wiese and Healy 1970; Penners and Koopal 1987; Ludwig, Peschel et al. 1988; Tufenkji and Elimelech 1999; Hahn, Abadzic et al. 2004; Hahn and O'Melia 2004; Tufenkji and Elimelech 2005), and some additional non-DLVO forces (Israelachvili and McGuiggan 1988; Israelachvili 1992). However, their relative roles in contributing to the discrepancy between theoretical prediction and the experimental results about the kinetics of deposition still remain unclear.

2.4 Deposition onto Heterogeneous Surfaces

2.4.1 Source and Description of Surface Heterogeneity

The study of deposition onto surfaces that are geochemically heterogeneous has captured significant attention not only because surface heterogeneity was one of proposed reasons suggested for the disparity between theory and observation in experiment in particle deposition, but also because many surfaces encountered in real environments are heterogeneous. Several mechanisms can be responsible for the development of surface heterogeneity of minerals including complexity of surface crystalline structure, complexity of chemical composition (Jaroniec and Madey 1988; Hiemenz and Rajagopalan 1997; Sposito 2008) and surface-bound impurities (Ryan and Gschwend 1992; Stumm, Morgan et al. 1996). A common source of charge heterogeneity for subsurface aqueous environment is oxide of certain metals such as iron, aluminum and manganese (Johnson, Sun et al. 1996). In fact it has been reported that several species of iron oxide are abundant in the soil environment. (Wang, White et al. 1993; Cornell and Schwertmann 1996) The importance of understanding the effect of surface heterogeneity, in the case of iron oxide for example, is that kinetics of particle deposition would be profoundly changed (Song, Johnson et al. 1994; Johnson, Sun et al. 1996). In the range of environmental pH, certain species of iron oxide bear positive charges (Cornell and Schwertmann 1996) while the silica surface is always negatively charged. This

means that the electrostatic field emanating from the silica collector would be distorted by the presence of iron oxide on the surface. Several attempts have been made to mathematically describe the effect of surface geochemical heterogeneity on the distribution of surface potential and double layer interaction (Richmond 1974; Richmond 1975; Schumann 1984; Schumann and D'Epenoux 1987; Kuin 1990; Miklavic, Chan et al. 1994). Experiments were also conducted to investigate the effect of the surface charge heterogeneity on adsorption of potential determining ions (Koopal and Van Riemsdijk 1989; Koopal, Dukhin et al. 1993) and it was in those studies that two models of charge distribution were proposed and distinguished: the random heterogeneous surface and the patch-wise heterogeneous surface. In the patch-wise model the surface coverage λ_i of type i patch (of potential ψ_i) is given by the probability density function:

$$p_i = p(\psi_i) = \lambda_i \quad \text{Eqn. 50}$$

In the random distribution model potential varies continuously along the surface. Assuming a normal distribution model with a mean value of ψ_0 and a standard deviation of σ , the surface potential probability density function can be expressed as:

$$p(\psi_i) = \frac{1}{\sigma\sqrt{2\pi}} \exp\left[-\frac{(\psi_i - \psi_0)^2}{2\sigma^2}\right] \quad \text{Eqn. 51}$$

2.4.2 Particle Deposition onto Heterogeneous Surface

The kinetics of particle deposition onto heterogeneous surface has been investigated both theoretically and experimentally (Vaidyanathan and Tien 1991; Song, Johnson et al. 1994; Song, Johnson et al. 1994; Johnson, Sun et al. 1996; Adamczyk, Siwek et al. 2001; Adamczyk, Weronki et al. 2002; Elimelech, Chen et al. 2003; Adamczyk, Jaszcz et al. 2005; Nazemifard, Masliyah et al. 2006). Using an inverse procedure of parameter estimation, Song and Elimelech (Song, Johnson et al. 1994) were able to identify the characteristic parameters for the surface charge heterogeneity from experimental results based on either the patch-wise model or the random distribution model. In addition, particle deposition becomes a transient process such that its kinetics varies over time due to the blocking of the favorable sites by the deposited particles (Song and Elimelech 1994). The phenomenon was modeled by relating the deposition rate to the rate of change of surface coverage with a dynamic blocking function (Johnson, Sun et al. 1996) modified from random sequential adsorption (Adamczyk, Weronki et al. 2002). Based on a model in which the heterogeneous sites are assumed to be spheres on the substrate surface, Adamczyk (Adamczyk, Siwek et al. 2002; Adamczyk, Weronki et al. 2002) was able to demonstrate, using Monte Carlo simulation, that the initial flux of deposition increases significantly with the site

coverage and the particle/site size ratio. Recent studies on particle deposition onto a surface with chemically micro-patterned heterogeneous surface reveals, both experimentally (Elimelech, Chen et al. 2003) and theoretically (Nazemifard, Masliyah et al. 2006), that when the characteristic dimension of the pattern is comparable to the particle size there exists a “hydrodynamic bump” effect so that the deposition rate would be significantly lower compared to that predicted by the patch model.

Although studies exist using a mixture of negatively charged uncoated quartz sands and positively charged quartz sands that are fully coated with either iron oxyhydroxide (Johnson, Sun et al. 1996) or aminosilane (Elimelech, Nagai et al. 2000) and the linear relationship between the attachment efficiency (α) and ratio of mixing (of the positively charged and negatively charged collectors) was proved with the aminosilane coated collectors, it might be questionable that whether such an introduction of the oppositely charged collectors can realistically represent the surface heterogeneity that often occurs locally on a single collector surface. Therefore, it might be helpful to revisit the similar problem using partially modified surface that might mimic the local heterogeneity more realistically. Perhaps more importantly, the heterogeneity parameter λ , which represents the fraction of surface for favorable deposition and was equivalent, in the existing studies, to the proportion of the ideal collector the surface of which was fully coated and positively charged, is hardly a practical parameter for a real environmental surface. It is thus useful to investigate the possibility of employing

common surface composition analysis techniques to facilitate the prediction of the affinity of nanoparticles for a heterogeneous surface by using the surface composition as a more pragmatic parameter to describe heterogeneity, which is the primary purpose of current study.

3. Materials and Methods

In this section we would explain in details the synthesis and characterization of the silver nanoparticles (AgNPs) and the heterogeneous collectors we used in this study. We would also explicate the detailed procedures and parameters of the column test as well as the determination of the attachment efficiency that represent the affinity between the nanoparticles and the surface in interest.

3.1 Synthesis and Characterization of Silver Nanoparticles

Suspensions of charged-stabilized AgNPs were prepared using the borohydride-reduction method (Creighton, Blatchford et al. 1979). Briefly, 10 mL of 1mM silver nitrate (Sigma Aldrich, St. Louis, MO) was added drop-wise to 30 mL of 2mM ice-chilled sodium borohydride (Fisher Scientific, Pittsburgh, PA). In this procedure the Ag^+ ions are reduced by BH_4^- to form AgNPs that are electrostatically stabilized by BH_4^- (or later BO_2^- as oxidized) ions adsorbed on the particle surface. The produced AgNPs were stable in suspension and were used as is without further purification for two reasons: First, for uncoated AgNPs it was infeasible to prevent aggregation during the washing procedure or to re-suspend the aggregated samples back to their primary particles' form; second, the volume of background electrolyte used in the subsequent experiments was overwhelmingly larger than that of the AgNPs suspension and thus the ionic strength of the AgNPs stock suspension as contributed by the residual ions would have

a negligible impact on the total ionic strength through out the whole range of ionic strengths tested. The UV-Vis spectrum of the AgNPs was scanned using a spectrophotometer (UV-Vis 2810, Hitachi, Pleasanton, CA) to confirm the existence of Surface Plasmon Resonance (SPR) characteristic of AgNPs. Both Transmission Electron Microscopy (FEI Tecnai G² Twin, Hillsboro, Oregon) and dynamic light scattering using a goniometer (ALV/CGS 3, Germany) were conducted to obtain size information of the AgNPs. The electrophoretic mobility (EM) of the AgNPs was measured using a Zeta-Sizer (Nanosizer ZS, Malvern Instruments, Worcestershire, U.K.). The EM measurements were conducted at a fixed ionic strength of 10^{-2} M as adjusted by NaNO₃ and at a variety of pHs ranging from 5 to 8.3 as adjusted by NaOH and HNO₃.

3.2 Preparations and Characterizations of Porous Media

3.2.1 Preparations of Porous Media

Spherical silicate glass beads (Potters Industries Inc. Berwyn, PA) were washed following a protocol by Espinasse (Espinasse, Hotze et al. 2007) to remove the organic and inorganic impurities on the glass beads' surface. The procedure for preparing iron oxide (FeO) coated glass beads (FeO-GB) largely follows that of Benjamin (Benjamin, Sletten et al. 1996) for coating silicate sand surface for arsenic removal. Two types of FeO-GBs were prepared—one with a higher surface coverage (FeO-GB-HC) and the other with a lower surface coverage (FeO-GB-LC). To prepare the FeO-GB with higher coverage (FeO-GB-HC), a mixture of 600 g glass beads (Potters Industries Inc.) and 80 mL of a 2.5 M FeCl₃ solution (Fisher scientific) was heated at 110 °C for 12 hours. The resulting wet slurry was sintered at 550°C for another 3 hours after which a dry mixture of blackish and reddish beads was formed. This mixture consisted of both iron oxide coated glass beads and particulate iron oxide. Beads between 300 µm and 400 µm were selected by sieving and the particulate iron oxide unassociated with the glass beads was removed by vigorous and extensive water flushing using a 300 µm mesh as support until the turbidity of the flow-through water was the same as that of the inlet water. The procedure for preparing FeO-GB with lower coverage (FeO-GB-LC) was similar with two exceptions: the slurry mixture was heated at 110 °C for 3 hours instead of for 12 hours and, the dry mixture after sintering was subject to extensive washing by 0.1 M nitric acid twice before the final stage of flushing with water. In both samples, the iron oxide formed at the surface was predominantly hematite (Cornell and Schwertmann 1996). The FeO-GBs prepared using these two methods were visually different in that the FeO-GB-LC had a lighter overall color than the FeO-GB-HC. It should be noted that even though FeO-GB-HC was tested to have higher FeO surface coverage than the FeO-

GB-HC, the silica surface was still only partially covered with FeO as revealed by both microscopic image and surface composition characterization.

3.2.2 Characterization of Porous Media

The glass beads (GB) and FeO-GBs were characterized with respect to the surface chemistry and morphology of these collectors. First, the surface potential (as approximated by the ζ potential) of the collectors were evaluated using streaming potential measurements (ZetaCad, CAD Instruments, France) which were conducted at the same solution chemistry as for the EM measurements mentioned above. X-ray photoelectron spectroscopy (Axis Ultra, Kratos Analytical, Chestnut Ridge, NY) was used to determine the surface elemental composition of the FeO-GBs prepared using two different methods. Because the size of the projection area of a collector was similar to the size of the sampling area (0.3mm×0.7mm), at least 30 measurements were conducted to generate representative results. The spectra data collected using XPS was processed by CasaXPS (Casa Software Ltd) to calculate the relative concentrations of Si and Fe on the surface. Finally, scanning electron microscopy (FEI XL30 FEG-SEM, Hillsboro, Oregon) was employed to observe the morphology of iron oxide coated surface.

3.3 Column Experiment and Determination of Attachment Efficiency

3.3.1 Column Experiment

The affinities between AgNPs and different surfaces were evaluated by measuring the removal of the AgNPs by a well-defined porous media comprised of the collectors of interest. The spherical collectors were packed into a chromatography column (C10/10, GE Healthcare, NJ) with an inner diameter of 10mm and a height of 6cm with the assistance of a height adaptor (GE Healthcare, NJ). Mild sonication using a sonication bath was applied to ensure that the column was tightly packed and that minimum porosity was attained. The background electrolyte solution was delivered by a single magnetic-drive gear pump (Cole-Parmer Instrument Company, Chicago, IL) at a flow rate of 0.94 mL/min which corresponded to a Darcy velocity of 0.02 cm/s in this system. The addition of AgNPs suspension was achieved by a syringe pump (Harvard Apparatus, Holliston, MA) at a flow rate of 0.04 mL/min that was negligible compared to the electrolyte flow rate. The electrolyte solution and the nanoparticle suspension were mixed in a Y-connector (BioChem Fluidics, UK) before the mixture entered the packed column. A diagram of the experimental set-up is provided in Figure 3. At least ten pore volumes (PV) of background electrolyte were passed through the column to equilibrate the surface of the porous media before conducting the deposition experiment.

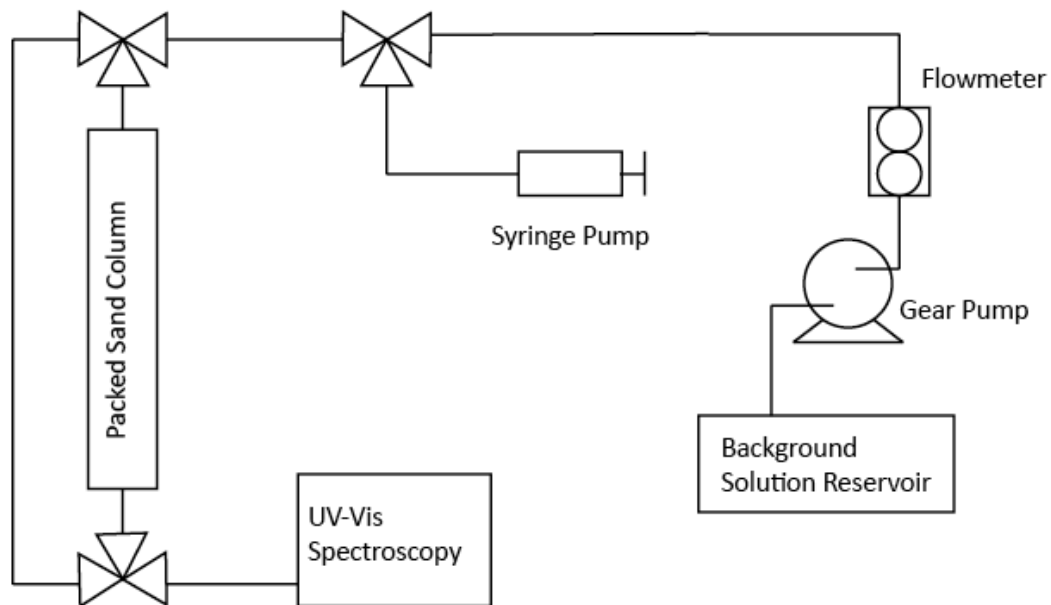


Figure 3: Diagram of a column test setup

The real time relative concentration of AgNPs was quantified by a UV-Vis spectrophotometer (UV-Vis 2810, Hitachi, Pleasanton, CA) with a flow module. The primary peak of the UV-Vis spectra for the AgNPs was at the wavelength of 399nm. A summary of the experimental parameters for column test is provided in Table7.

Table 7: Parameters for Column Experiments

Parameters	Values
Packed media length	6cm
Column inner	1cm
Media porosity	0.378
Darcy velocity	0.02 cm/s
Particle suspension /Electrolyte volume ratio	0.043
UV-Vis monitoring wavelength	399nm

The GB and the FeO-GB-HC were respectively used as collectors for column tests at both pH 5 and pH 8.3 with a variety of ionic strengths to assess and compare the affinity of AgNPs for these two different porous media under various conditions of solution chemistry. To study the effect of mineral heterogeneity of porous media on attachment efficiency and to evaluate the hypothesized linear relationship between the attachment efficiency and surface composition, the FeO-GB-HC was mixed with uncoated GB at different mass ratios for column tests at a pH of 5 and an ionic strength of 0.01 M. With the same solution chemistry, the affinity of uncoated AgNPs in a porous medium composed of FeO-GB-LC was also measured. The attachment efficiency thereby obtained was coupled with the XPS data to evaluate the validity of using surface composition analysis for conditional prediction of attachment efficiency.

3.3.2 Determination of Attachment Efficiency

The deposition experiments measured the concentration of AgNPs passing through the column which, after accounting for fluid velocity, collector size, temperature and other physical factors that enter into the calculation of the collector efficiency, η_0 , allows for the calculation of the attachment efficiency of between the particle and the collector surface. The attachment efficiency can be defined as the probability of successful attachment per particle-collector collision and is theoretically dependent on the composition, size and surface chemistry of both the collector and nanoparticles as well as the solution chemistry. It can be calculated using the following equation obtained by integrating, over the column length, the mass balance equation describing a differential volume of porous medium (Yao, Habibian et al. 1971):

$$\alpha = -\frac{1}{\eta_0} \frac{2d}{3(1-\varepsilon)L} \ln \frac{C_{eff}}{C_{inf}} \quad \text{Eqn. 36}$$

where d_c is the diameter of the collectors in the porous medium, ε is the packing porosity, L is the length of the column, C_{eff} and C_{inf} are the particle concentrations at the effluent and influent respectively, and η_0 is the single collector contact efficiency. The single collector contact efficiency η_0 describes the efficiency of particle contacts with the collector occurring primarily by Brownian diffusion, interception and gravitational sedimentation. The collector efficiency can be calculated in closed form equations

obtained by correlating simulation results with a set of non-dimensional parameters. (Tufenkji and Elimelech 2004) For the case of non-aggregate particles of nano-scale, Brownian diffusion, η_D , is the dominant mechanism (Yao, Habibi et al. 1971) by which particles come in contact with a collector ($\eta_D \approx \eta_D$). Because van der Waals (vdW) force is a body force, although the surface of collector is partially covered with iron oxide, it is still reasonable to use the Hamaker constant between silica and Ag in water as medium ($A_{Ag-w-si}$) for the correlation. Based reported values of A_{Ag-Ag} (Bargeman and Van Voorst Vader 1972) and A_{Si-Si} (Bergstrom 1997), the Hamaker constant $A_{Ag-W-Si}$ was calculated to be 1.97×10^{-20} .

4. Results and Discussion

In this section we would present the results of experiment as described in section 3 and discuss the implication of these results. We would start by discussing the properties of the silver nanoparticles (AgNPs) and the GB and FeO-GB collectors, then focus on the deposition kinetics of AgNPs for different porous media under different conditions, and finally attempt to establish a correlation between the AgNPs-Collector affinity and the surface composition of the collectors.

4.1 Properties of Silver Nanoparticles

The AgNPs suspension prepared had a clear bright yellow color as confirmed by a UV-Vis spectrum that peaked at 399 nm. The hydrodynamic radius of the AgNPs was measured to be 12.09 ± 1.01 nm by dynamic light scattering, which was around twice the average particle size as given by TEM image analysis. The TEM image, size distribution based on TEM image analysis, and UV-Vis spectrum for the AgNPs, are given in Figure 4, Figure 5, and Figure 6 respectively.

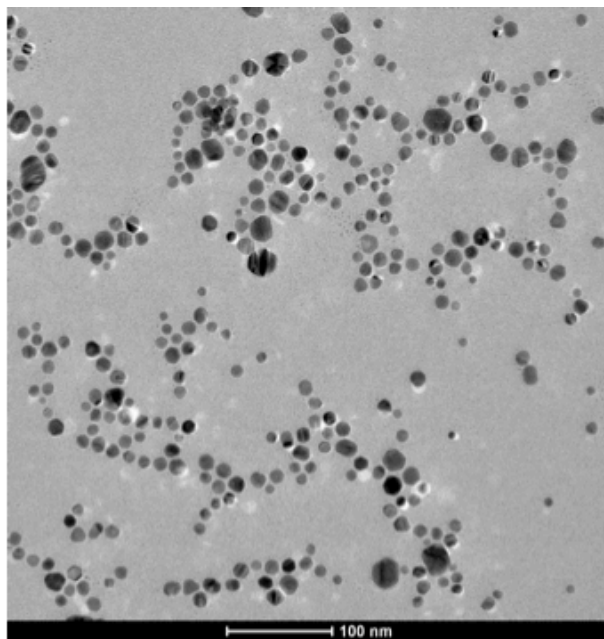


Figure 4: Transmission electron microscopy of charge-stabilized silver nanoparticles (AgNPs)

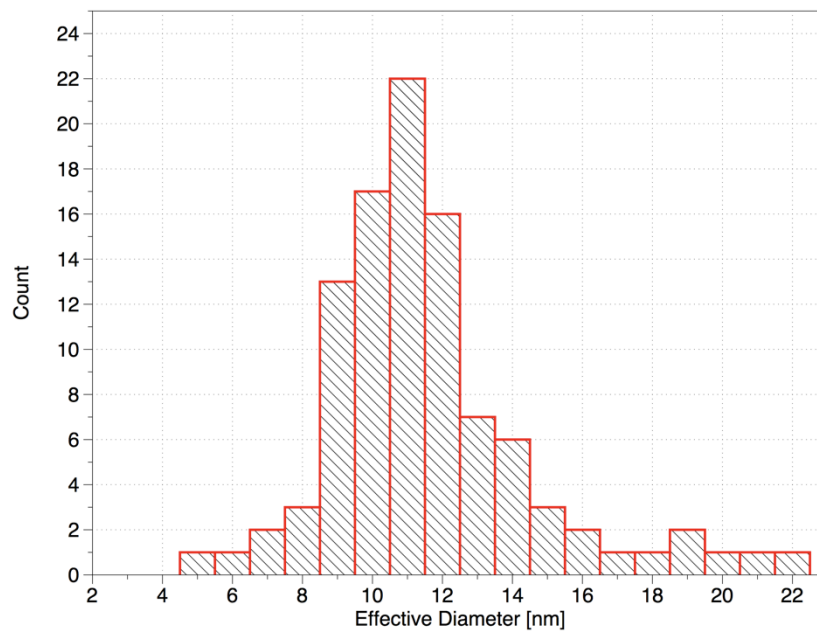


Figure 5: AgNPs size (diameter) distribution from TEM image analysis

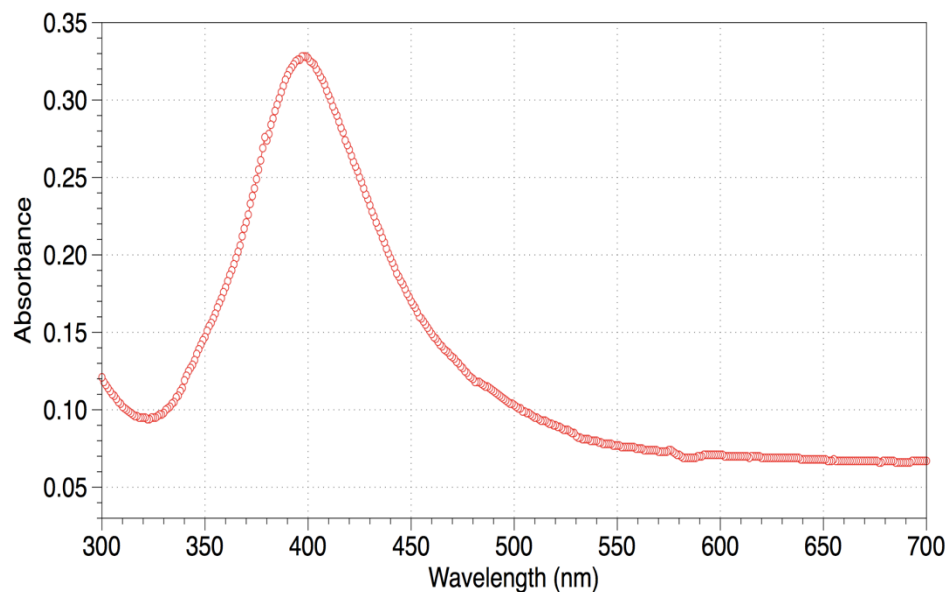


Figure 6: UV-Vis spectrum of charge-stabilized AgNPs

The hydrodynamic size instead of the actual size observed by TEM was used in calculating the single collector contact efficiency η_0 because it is more relevant to Brownian transport of the AgNPs. The AgNPs suspension was stable throughout the timeframe of the experiment as measured by hydrodynamic size and UV-Vis spectroscopy. No change of color or evidence of sedimentation was observed.

4.2 Morphology and Composition of Collector Surfaces

The FeO coating on the surface of the FeO-GB-HC was patchy and inhomogeneous as can be observed in the scanning electron microscope (SEM) image shown in Figure 7. Two representative XPS spectra, one for FeO-GB-HC and the other for FeO-GB-LC, are presented respectively on Figure 8 which shows an apparent difference in the height of the Fe-2P peaks on the spectra. The ratio Fe/(Fe+Si) as a measure of surface abundance of Fe compared to Si was 25.34 ± 3.04 % for FeO-GB-HC and 6.84 ± 1.87 % for the FeO-GB-LC based on more than 30 XPS measurements for each type of samples. Although it can be observed from the SEM images that the iron oxide coatings were visually inhomogeneous and the surface coverage appears to vary from one bead to another, the Fe/(Fe+Si) ratios given by XPS measurement were relatively consistent for all the examined collectors. It should also be noted that relative surface concentration of Fe as measured by XPS was higher than the patchy coverage observed visually, which implies that even the “uncovered area” might in fact be partially associated with Fe in certain forms.

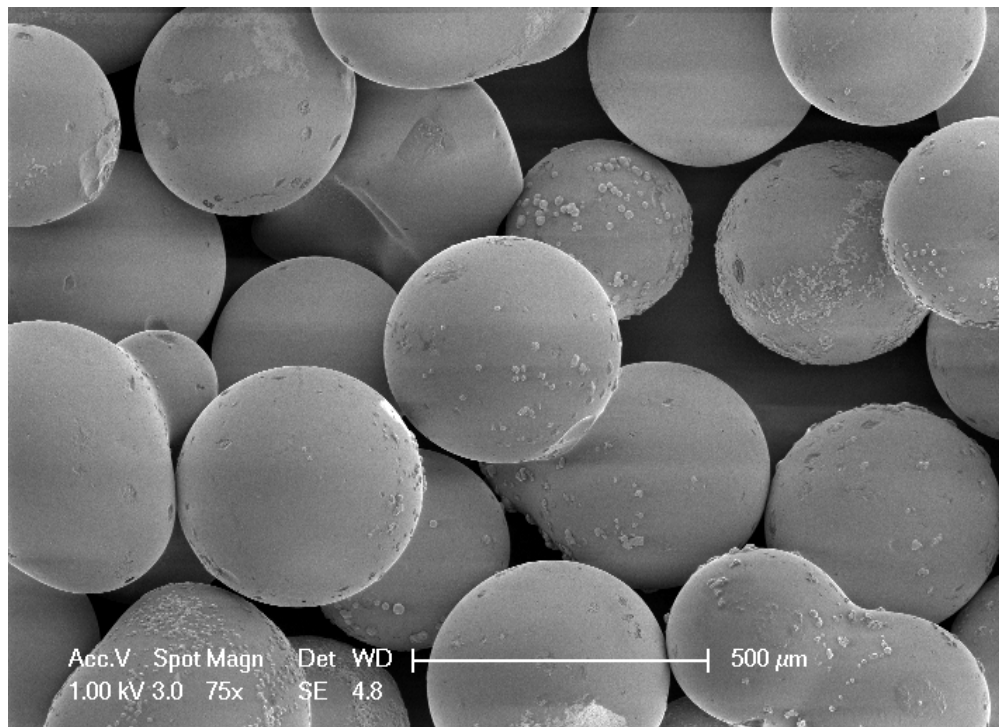


Figure 7: Scanning electron microscopy image of FeO-GB-HC

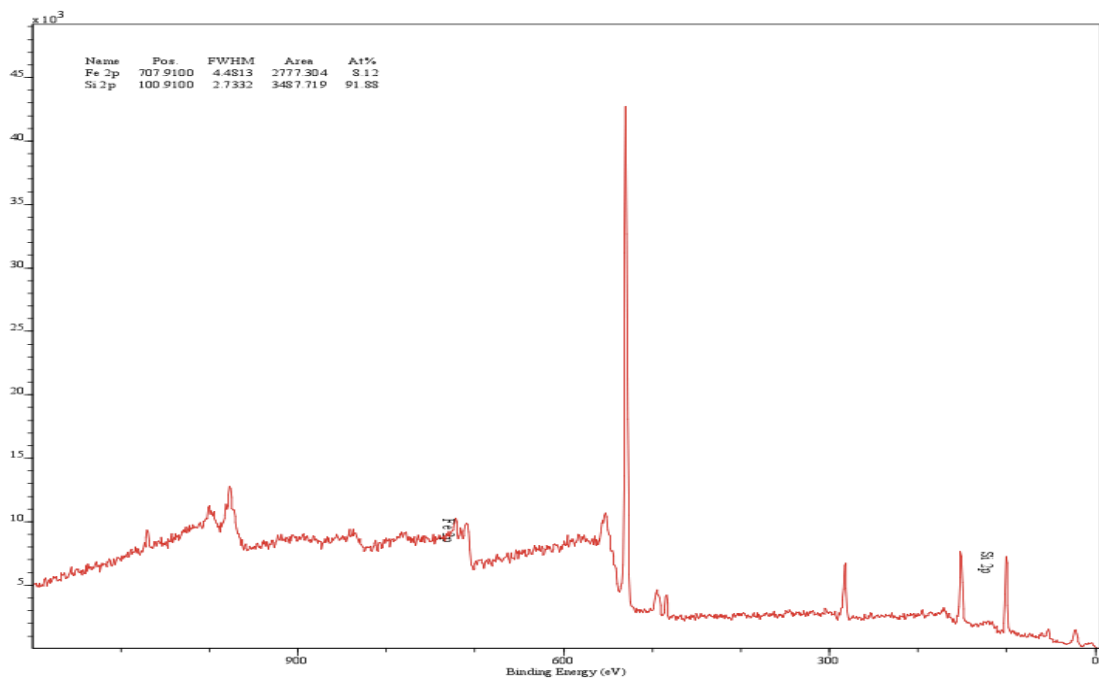
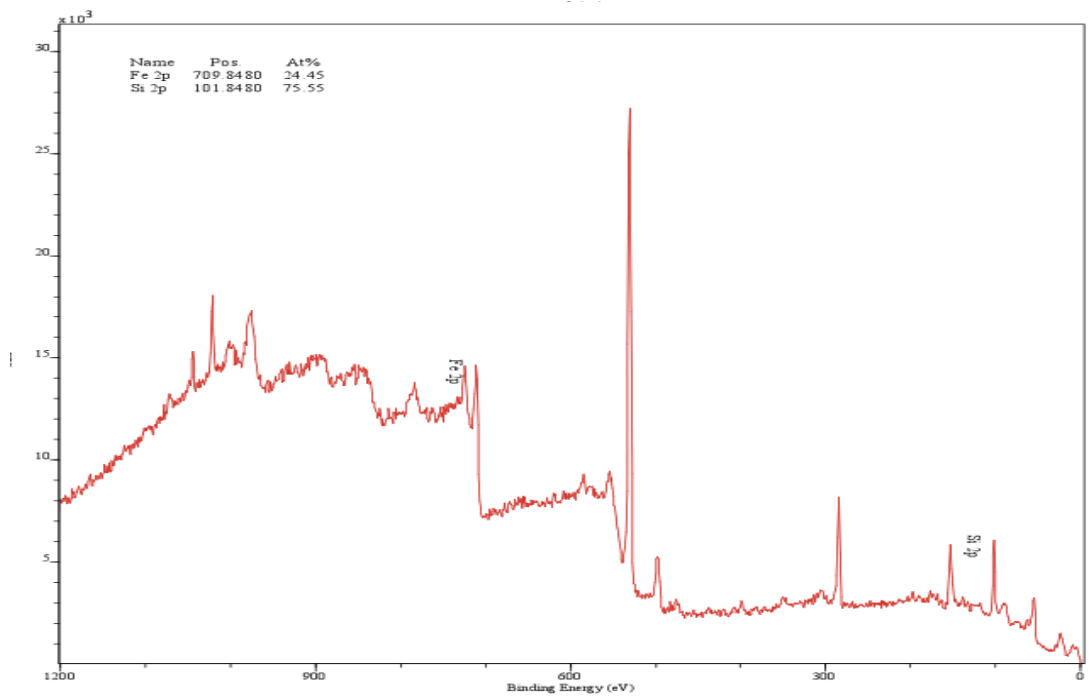


Figure 8: XPS spectra of FeO-GB-HC (top) and FeO-GB-LC (bottom)

4.3 Surface Chemistry of AgNPs and Collectors

The zeta (ζ) potentials of the AgNPs, GB, and FeO-GB-HC were all negative from pH 5 to pH 8.3 as shown on Figure 9. Comparatively speaking, the ζ potentials of AgNPs were lower (less negative) than that of the collectors. However, such a comparison should be made with caution because the ζ potentials of the nanoparticles were measured using electrophoresis while those of the collectors were measured using streaming potential technique, although study exists showing that these two techniques would essentially lead to the same results (Silvert, Herrera-Urbina et al. 1997). It should also be noted that the FeO-GB-HC was still of relatively high negative charge even when pH=5—a pH considerably lower than the reported PZC for hematite (Kosmulski 2001), which implies that the negatively charged silica patches have a significant contribution in determining the surface potential under this condition.

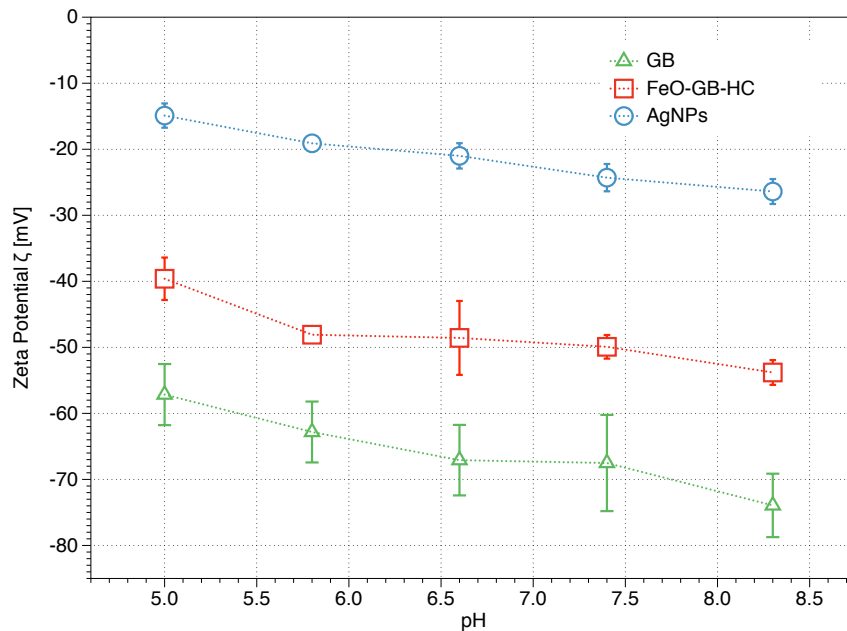


Figure 9: Zeta potentials of AgNP, GB, and FeO-GB-HC at various pHs (ionic strength was fixed at 0.01 M)

4.4 Effect of pH and Ionic Strength on Particle Deposition

Figure 11a and 11b show the representative breakthrough curves for AgNPs at pH 5 and pH 8.3 with a range of ionic strengths in porous media of GB and FeO-GB-HC respectively. In both porous media, attachment of the AgNPs increased with increasing NaNO_3 concentration due to electrical double layer (EDL) compression. An obvious difference was observed between the shapes of the breakthrough curves (Figure 13) obtained using different porous media. With the uncoated GB as the porous medium, the effluent concentration of AgNPs reached a plateau soon after injection and remained

constant until the termination of injection. The breakthrough curves in this case were similar to that of the tracer. However, for the porous medium of FeO-GB-HC, a flat plateau was not observed even after 3 PVs of injection. The effluent concentration continued to increase gradually as more and more AgNPs deposited onto the collector surface. This phenomenon can be explained by the dynamics of deposition in which the negatively charged AgNPs blocked the positively (or less negatively) charged sites so that local favorable deposition may be attenuated and eventually replaced by electrostatic repulsion over longer time-frames due to surface charge reversal. (Johnson, Sun et al. 1996)

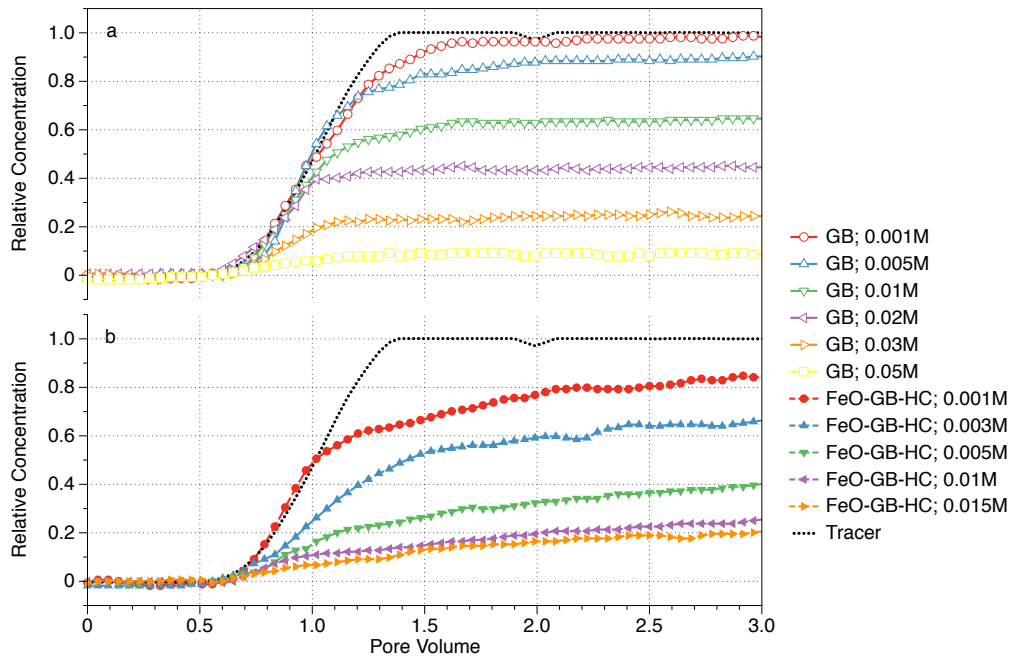


Figure 10: Representative breakthrough curves for AgNPs deposition in GB (a) and FeO-GB-HC (b) at pH 5

The attachment efficiency α calculated from the $C_{\text{eff}}/C_{\text{inf}}$ obtained from experimental breakthrough curves at two different values of pHs (5.0 and 8.3) and various ionic strengths for two porous media are shown in Figure 10. Qualitatively consistent with standard DLVO theory, the attachment efficiency increased with increasing ionic strength as the diffuse layer was compressed and the EDL interaction was weakened. At pH 8.3, both the GB and iron oxide portion of FeO-GB-HC were negatively charged, as this pH is greater than PZCs of both silica and hematite. Theoretically, the GB would be more negatively charged than the FeO-GB-HC since the PZC for GB was further away from the solution pH than that of the FeO and therefore at the same ionic strength the attachment efficiency between AgNPs and FeO portion of the FeO-GB-HC should be higher than that between AgNPs and GB. However, the differences in attachment efficiencies between two porous media at ionic strengths up to 0.02M were not statistically significant. A drastic enhancement in AgNPs removal by the FeO-GB was observed when the ionic strength was increased to 0.03 M, probably due to the elimination of energy barrier between the AgNPs and the FeO fraction of the collector surface. At pH 5.0, the affinity of AgNPs for FeO-GB was noticeably greater than that for GB even at relatively low ionic strength. Because the PZC of hematite was higher than pH 5.0 it should be expected that the FeO fraction should be positively charged at pH 5.0 and thus the deposition of nanoparticles onto the FeO fraction should be favorable. However, the measured overall attachment efficiency was significantly

lower than that predicted by assuming that 25% of the surface was covered by hematite and that the hematite fraction would lead to favorable deposition. One possible explanation would be that the AgNPs approaching the positively charged hematite patches might experience a “hydrodynamic pump” effect that may occur during particle deposition onto a surface with micro-patterned charge heterogeneity (Elimelech, Chen et al. 2003; Nazemifard, Masliyah et al. 2006). Another possibility is that although the XPS measurement gave a value of 25.34 ± 3.04 % for Fe/(Fe+Si) of the FeO-GB-HC, the fraction of surface area covered by large hematite patches might be significantly smaller than 25%. Part of the total surface Fe concentration detected by XPS might be contributed by the iron Fe located either in the uncovered area as $\equiv\text{Si-O-Fe}$, or underneath the uncovered area as a result of isomorphous substitution. Therefore, the effective FeO patches leading to favorable deposition might be in fact smaller than that suggested by XPS measurements.

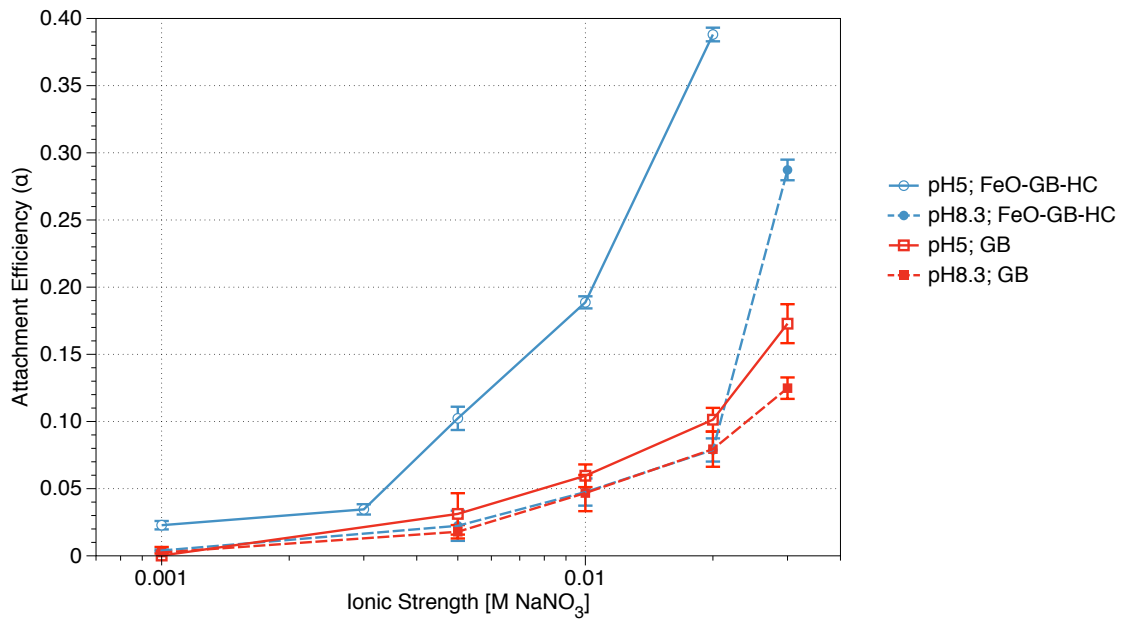


Figure 11: Attachment efficiencies between AgNPs and GB (FeO-GB-HC) at various ionic strengths (0.001 M-0.03 M) and pHs (5 and 8.3)

4.5 Relative Insignificance of Zeta Potential ζ

It is tempting to simply apply the classic DVLO theory using measurable global parameters such as ionic strengths and the surface potentials of the particles and the collectors to predict the attachment efficiency α between the particle and the collector surface. Let alone the some intrinsic inadequacies of DLVO theory even in modeling the particle deposition onto a homogeneous surface,(Elimelech and Omelia 1990) using DLVO theory with the ζ potential of a heterogeneous surface would introduce further problems, which has been elucidated by Elimelech et al. (Elimelech, Nagai et al. 2000)

using a mixed porous medium composed of quartz sand (negatively charged) and silylated quartz sand (positively charged) for deposition experiments. The authors showed that the deposition kinetics was determined primarily by the extent of heterogeneity and that using ζ of the collector surface for prediction would lead to erroneous results. Our experimental observation of AgNPs deposition onto a collectors of local heterogeneity (i.e. patchwise heterogeneity on a single collector as compared to column scale heterogeneity) also supports the aforementioned argument. Even without conducting a detailed calculation employing the interaction force boundary layer approximation, (Spielman and Friedlander 1974) it can be shown that

$\alpha \propto e^{-V_{Tot}/k_B T}$ (Elimelech and Omelia 1990) does not hold if the total interaction energy

V_{Tot} is evaluated using the measured ζ potential. We used expression by Gregory

(Gregory 1981) for calculating vdW interaction potential and the linear-superposition-

approximation-based improved analytical expression for calculating sphere-plate EDL

interaction (Lin and Wiesner 2010). Figure 12 presents the $\text{Log}\alpha_{exp}$ vs. barrier of the total

interaction energy ($V_{Tot}/k_B T$) based on column test and zeta potential measurement

results. If using the classic DLVO theory with ζ potentials were a valid measure to

predict the attachment efficiencies, all the data points on Figure 12 should have fallen

into a straight line, which was not observed. The starred data points on Figure 13 refer to

the measurement on GB only (assumingly homogeneous surface). Theoretically, the

dashed line (reference line) connecting the starred data points is where valid DLVO

predictions would be located. When pH=5 (below the PZC of FeO), all the data points are above the reference line, meaning that the particle-collector affinity was higher than that predicted using DLVO theory with the apparent ζ potential of the heterogeneous collectors. For the mixed column at pH5, the higher the degree of introduced heterogeneity, the higher the extent to which the data points deviated from the reference line because a higher fraction of surface was available for favorable deposition.

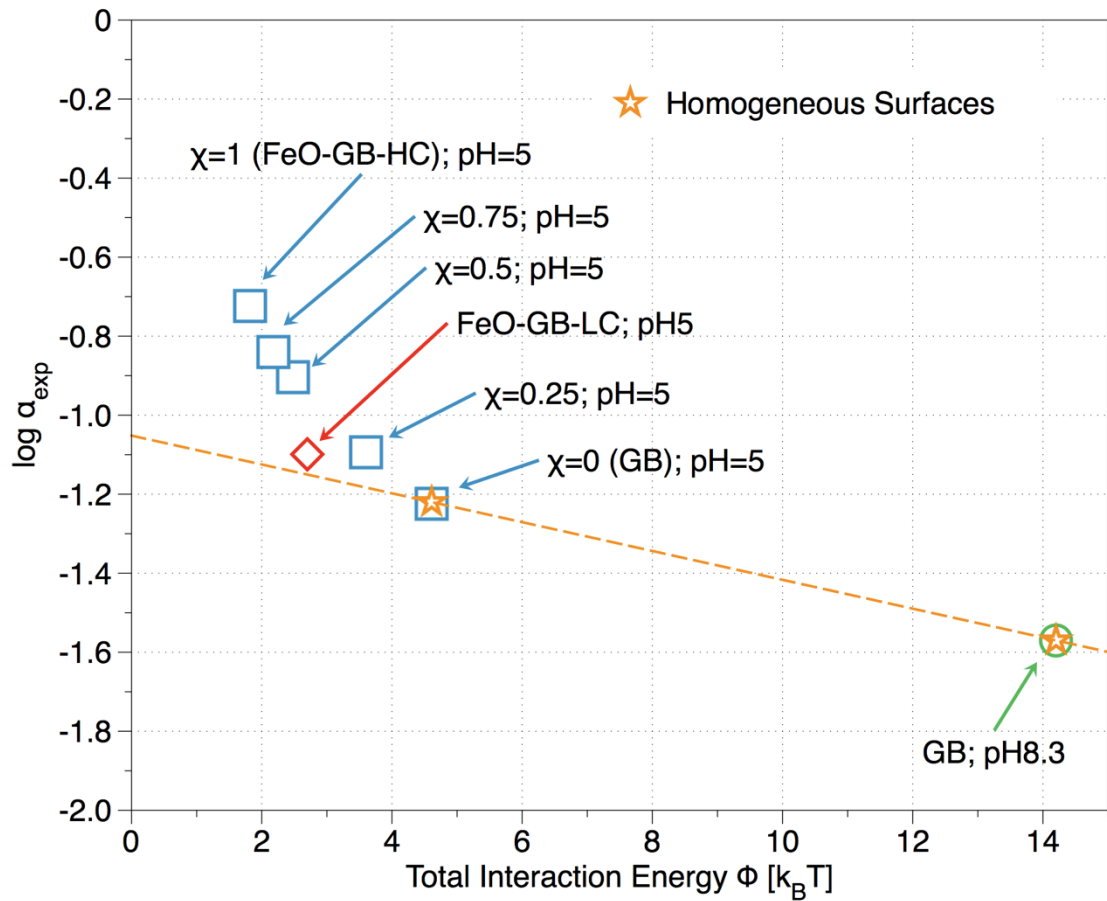


Figure 12: Log α_{exp} vs. Φ_{Total} for certain deposition experiments. The α_{exp} is attachment efficiency obtained from column experiments. The energy barrier is calculated using the classic DLVO theory with the measured ζ potentials of the AgNPs and the collectors in the solution chemistry of corresponding experiments. χ is

the mass ratio of FeO-GB-HC in a medium composed of a mixture of GB and FeO-GB-HC. All data points were collected with ionic strength fixed at 0.01 M.

4.6 Correlation between Attachment Efficiency and Surface Composition of Heterogeneous Surfaces

To evaluate the affinity between AgNPs and other heterogeneous surface with known composition (i.e. the percentages of FeO and silica on surface in our case), it is necessary to understand the effect of the surface composition on the affinity of the AgNPs for the porous medium. The simplest possibility would be a linear relationship in which the affinity of a given type of nanoparticle in a heterogeneous porous medium composed of multiple types of collector surfaces is expressed as a composition-weighted average of the affinities of that type of nanoparticle for each of the individual types of collectors comprising the heterogeneous medium (Song, Johnson et al. 1994; Johnson, Sun et al. 1996). To test such a linear relationship for the current system, a series of heterogeneous media of varying surface compositions were prepared by mixing the GB and FeO-GB-HC at different mass ratios to evaluate the affinity of the AgNPs for such porous media while the solution chemistry was fixed at pH 5.0 and an ionic strength of 0.01M. As shown on figure 13, there was indeed a strong correlation ($R = 0.992$) between the affinity of AGNPs for the heterogeneous media and the mass percentage of the FeO-GB-HC. Similar evidence has been reported in literature for a system using a mixture of uncoated silica beads and beads that are fully coated with aminosilane (Elimelech, Nagai et al. 2000) .

Also measured was the AgNPs affinity for the FeO-GB-LC which is of lower FeO fraction and is heterogeneous only on a collector scale. Comparing the Fe/Si compositions from XPS measurement between FeO-GB-HC and FeO-GB-LC, it was possible to assign an equivalent mass ratio of FeO-GB-HC to the FeO-GB-LC, viewing the FeO-GB-LC as a mixture of FeO-GB-HC and GB, to quantify the surface composition of FeO-GB-LC for the purpose of predicting the affinity of AgNPs for these media. The compositional data from XPS and the attachment efficiencies from column test are presented also on Figure 13. Both the proportion of Fe and the attachment efficiency for FeO-GB-LC was between that of GB and FeO-GB-HC. Quantifying the surface composition of FeO-GB-LC using the mass ratio of FeO-GB-HC, it was calculated that the Fe proportion of the FeO-GB-LC surface was equivalent to a FeO-GB-HC mass ratio of 0.27 ± 0.08 in a FeO-GB-HC/GB bi-component porous medium. The fitting equation relating the overall attachment efficiency and the mass ratio of FeO-GB-HC in a heterogeneous column for this case was found to be $\alpha = 0.1289\chi + 0.055$, where α was the attachment efficiency between AgNPs and χ the FeO-GB-HC mass ratio of the bi-component medium. Using this equation and an equivalent χ of 0.27 ± 0.08 for FeO-GB-LC, the attachment efficiency α for the FeO-GB-LC was predicted to be 0.089 ± 0.01 which was different from the experimentally measured attachment efficiency α_{exp} by only 11%. Considering the fact that the sampling area for XPS with our instrument was only $0.7\text{mm} \times 0.3\text{mm}$ which is insufficient to cover two collectors at a time so that the

uncertainty associated with surface composition measurement is appreciable, it can be concluded that the α_{exp} agreed with prediction satisfactorily.

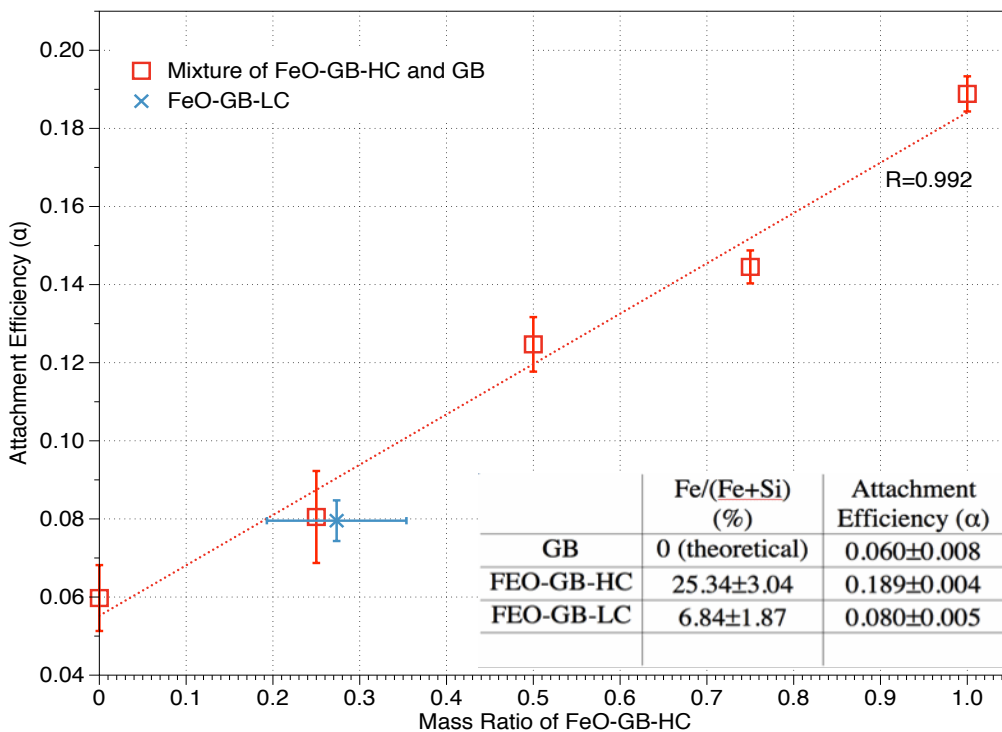


Figure 13: Attachment efficiencies of AgNPs for bi-component porous media composed of HB and FeO-GB-HC mixed at different ratios and for a mono-component porous medium composed of FeO-GB-LC. All experiments were conducted at an ionic strength of 0.01M and a pH of 5.

In addition to correlating the surface composition and the global attachment efficiency obtained from column tests, local evidence was also observed to further support the hypothesized linear correlation between the composition of a surface fraction and the affinity of the AgNPs for that fraction. FeO-GB-HCs were used as collectors in columns with a background electrolyte of 0.01 M and pH 5 and a flow rate identical to that used

in all other column tests conducted. One milliliter of AgNPs suspension was allowed to flow through the column before the FeO-GB-HC beads were collected for XPS measurement. Due to the longitudinal distribution of the AgNPs concentration in a column, only a thin slice of the porous medium was sampled to ensure that the FeO-GB-HCs for XPS measurement were all located at the same longitudinal position so as to avoid systematic error. Not only the Fe and Si elements but also the Ag element were analyzed to obtain a Fe/Si/Ag profile for each measurement. Because the FeO coating on the collectors was inhomogeneous and each measurement sampled only one to two collectors, a relatively wide spectrum of relative Fe concentration was obtained ranging from 16.77% to 30.63% for 22 measurements in which the relative Ag concentration ranged from 0.18% to 0.55%. The observed linear correlation between attachment efficiencies is reflected in a linear mapping between the relative Fe concentration and the relative Ag concentration on the collector surface as shown in Figure 14. The amount of the AgNPs retained on the collector surface increases linearly with the abundance of FeO on the collector surface.

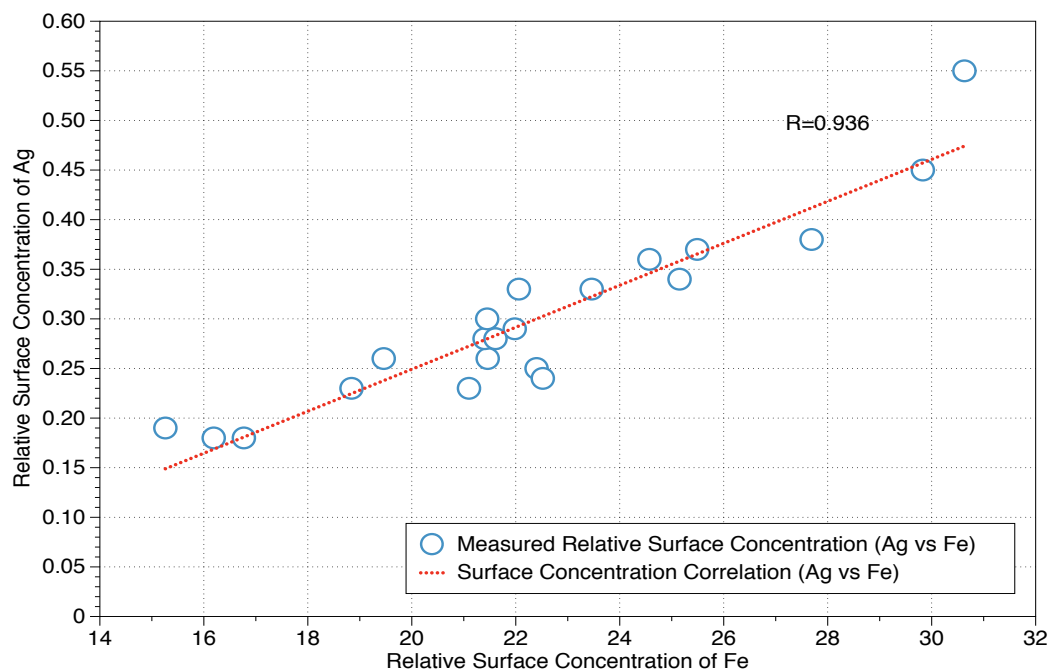


Figure 14: Correlation between the local relative concentrations of Fe and of Ag based on XPS composition analysis. FeO-GB-HC sample collectors were taken carefully from the same longitudinal position in a column that 1 mL of AgNPs passed through.

5. Conclusion

It was shown in this study through column experiments that the affinity of AgNPs for a surface is not only affected by the solution chemistry such as pH and ionic strength as DLVO theory predicted, but also by the geochemical heterogeneity of the collector surface. It was also shown that heterogeneity in the deposition context is relative, that the heterogeneous surface effect would be more salient when the pH becomes such that the charge states of the different surface portions are significantly different (either of different signs or of a same sign but to very different extents) and there thus exist significant different affinities for the same nanoparticles for different portions of the heterogeneous surface. Applying DLVO theory with the measured zeta potential of the collector surface is inappropriate in the case of a heterogeneous surface for the zeta potential as a global parameter fails to take into account the details of local surface heterogeneity. It is possible, however, to estimate the attachment efficiency between a nanoparticle and a heterogeneous surface given the following two pieces of information are known: (1). attachment efficiencies of one type of nanoparticles for the reference homogeneous surfaces or heterogeneous surfaces of known composition under a given solution chemistry; (2) the surface composition of the heterogeneous surface the kinetics of deposition onto which we are interested in. This finding might be helpful especially to the mobility assessment of nanoparticles in a porous medium of varying relative surface composition (i.e. surface of varying proportions of the same

components). Instead of gathering the zeta potential data at different sampling points for affinity prediction based on DLVO theory, it might instead be more reasonable to measure experimentally the affinity of the interested nanoparticles for several reference surfaces of known composition and then estimate such affinity elsewhere based on the location-dependent composition of the heterogeneous surface.

6. Work

This study focused on the deposition of charge-stabilized nanoparticles (as compared to sterically or electrosterically stabilized nanoparticles) onto an uncoated surface without the presence of the natural organic matter (NOM) which would significantly affect the particle deposition kinetics. Such a system under study is relative simple but it might be considered to ideal to be very environmentally relevant. It is very likely that more nanoparticles modified by polymeric surface coatings would enter our environmental system not only because they are in general more stable than the uncoated nanoparticles but also because they share a higher production volume due to that enhanced stability. Further more, NOM is ubiquitous in the aquatic systems and the presence would alter the particle-surface interaction in a way that is system-dependent. Whether a linear correlation between nanoparticles and the surface composition of a heterogeneous surface in the presence of NOMs, or engineered surface coatings, or both, remains unclear and requires further efforts to answer. In addition, the heterogeneity studied in this work only involves two components. It might be interesting to investigate the same problem but with a heterogeneous surface of more components to test whether the linear correlation would still hold. Finally, the surface in the current study is only heterogeneous with respect to surface charge while in reality other types of heterogeneity such as surface hydrophobicity/hydrophilicity would also exist.

Extending the linear correlation from the charge aspect to other realms would render it more universal and thus more useful.

Appendix A: Nomenclatures

General	
k_B	Boltzmann constant
g	Gravitational constant
T	Temperature
e	Electron charge
t	Time
N_A	Avogadro number
For molecular van der Waals interaction	
Φ_D	Potential of Debye interaction
Φ_K	Potential of Keesome interaction
Φ_L	Potential of London interaction
h	Plank's constant
ν	Characteristic vibrational frequency of electrons
$\alpha_0 (\alpha_{0,1}, \alpha_{0,2})$	Polorizability of molecules
x	Separation between dipoles centers
ϵ_0	Vacuum permittivity
ϵ_r	Relative permittivity
μ_1, μ_2	Dipole moment
β^*	Interaction parameter
ρ	Density of particle
M_w	Molecular weight of particle

For macrobodies van der Waals interaction

A_h	Hamaker constant
$a_p, (a_{p,1}, a_{p,2})$	Radius of (spherical) particle
d_p	Diameter of (spherical) particle
d	Separation between particles or between a particle and a plate
δ	Thickness of plate
$V_{vdW, sp}$	vdW interaction between a sphere and a plate
λ	Characteristic wavelength of vdW interaction
A_{ijk}	Hamaker constant for vdW interaction between i and k in a medium of j
A_{ij}	Hamaker constant for vdW interaction between i and j in vacuum

For electrical double layer interaction

Ψ	Electrical potential
ρ^*	Charge density (C/m ³)
z_i	Valence of ionic species i
$n_{i,\infty}$	Bulk concentration of ionic species i
κ	Debye constant
r	Distance away from a spherical particle center
$V_{pp}(L)$	EDL interaction between two infinite flat plates of separation L
$V_{sp}(d)$	EDL interaction between a sphere and a plate of separation d
$V_{ss}(H_0)$	EDL interaction between two spheres of separation H_0
$\psi_s (\psi_p)$	Surface potential of sphere (plate)
V_{vdW}	Potential of vdW interaction
V_{EDL}	Potential of EDL interaction
V_{Born}	Potential of Born repulsion

V_{Tot}	Total potential of interaction
σ_C	Collision diameter (in Born repulsion)

For particle stability and particle transport

W	Stability ratio
α	Attachment efficiency
η	Single collector efficiency
η_0	Theoretical single collector efficiency
K_F	Pseudo-first-order rate constant
C	Generic concentration
\vec{v}	Flow velocity
U	Darcy velocity of the flow in a porous medium
D	Diffusion coefficient of particles
m	Particle mobility (under driving force ∇V_{Tot})
ε	Porosity of the column
d_c	Diameter of spherical collector
C_{eff}	Effluent concentration (of particles)
$C_{eff,fav} (C_{eff,unfav})$	Effluent concentration under favorable (unfavorable) condition
C_{inf}	Influent concentration (of particles)
L	Length of the column
U	Darcy velocity of the flow
ρ_p	Particle density
ρ_w	Water density
μ	Kinematic viscosity of water
η_D	Theoretical single collector efficiency by diffusion mechanism
η_I	Theoretical single collector efficiency by interception mechanism

η_G	Theoretical single collector efficiency by gravitational sedimentation mechanism
N_R	Aspect ratio
N_{Pe}	Peclect number
N_{vdW}	vdW number
N_{gr}	Gravitational number
N_A	Attraction number
N_G	Gravity number

For surface heterogeneity description

λ_i	Surface coverage of species i (of surface potential of Ψ_i) or heterogeneity parameter
σ	Standard deviation of surface potential distribution
Ψ_i	Surface potential
Ψ_0	Mean of surface potential distribution
χ	Surface coverage of the positively charge species in a bi-component system

Appendix B: Abbreviations

AgNPs	Silver nanoparticles
PZC	Point of zero charge
DLVO	Derjaguin-Landau-Verwey-Overbeek (Theory)
vdW	van der Waals (interaction)
AWI	Air water interface
EDL	Electrical double layer (interaction)
PB	Poisson-Boltzmann (equation)
LSA	Linear superposition approximation
CP	Constant potential
CC	Constant charge
CDC	Critical deposition concentration
SPR	Surface Plasmon resonance
EM	Electrophoretic mobility
GB	Glass beads
FeO-GB	Iron oxide coated glass beads
FeO-GB-HC	Iron oxide coated glass beads of high (FeO) coverage
FeO-GB-LC	Iron oxide coated glass beads of low (FeO) coverage
SEM	Scanning electron microscopy
XPS	X-ray photoelectron spectroscopy
TEM	Transmission electron microscopy

Reference

- Abudalo, R., Y. Bogatsu, et al. (2005). "Effect of ferric oxyhydroxide grain coatings on the transport of bacteriophage PRD1 and *Cryptosporidium parvum* oocysts in saturated porous media." Environmental Science & Technology **39**(17): 6412.
- Adamczyk, Z. (1983). "Particle transfer to solid surfaces." Advances in colloid and interface science **19**(3): 183-252.
- Adamczyk, Z., K. Jaszcz, et al. (2005). "Irreversible adsorption of particles on heterogeneous surfaces." Advances in colloid and interface science **118**(1-3): 25-42.
- Adamczyk, Z., B. Siwek, et al. (2001). "Kinetics of colloid particle adsorption at heterogeneous surfaces." Langmuir **17**(15): 4529-4533.
- Adamczyk, Z., B. Siwek, et al. (2002). "Irreversible adsorption of colloid particles at heterogeneous surfaces." Applied surface science **196**(1-4): 250-263.
- Adamczyk, Z., P. Weroński, et al. (2002). "Colloid particle adsorption at random site (Heterogeneous) surfaces." Journal of Colloid and Interface Science **248**(1): 67-75.
- Baker, C., A. Pradhan, et al. (2005). "Synthesis and antibacterial properties of silver nanoparticles." Journal of Nanoscience and Nanotechnology **5**(2): 244-249.
- Bargeman, D. and F. Van Voorst Vader (1972). "Van der Waals forces between immersed particles." Journal of Electroanalytical Chemistry **37**: 45-52.
- Benjamin, M., R. Sletten, et al. (1996). "Sorption and filtration of metals using iron-oxide-coated sand." Water Research **30**(11): 2609-2620.
- Bergstrom, L. (1997). "Hamaker constants of inorganic materials." Advances in colloid and interface science **70**: 125-169.
- Bhattacharjee, S. and M. Elimelech (1997). "Surface element integration: a novel technique for evaluation of DLVO interaction between a particle and a flat plate." Journal of Colloid and Interface Science **193**(2): 273-285.

- Boller, M. and M. Kavanaugh (1995). "Particle characteristics and headloss increase in granular media filtration." Water Research **29**(4): 1139-1149.
- Borm, P., D. Robbins, et al. (2006). "The potential risks of nanomaterials: a review carried out for ECETOC." Particle and Fibre Toxicology **3**(1): 11.
- Bosetti, M., A. Masse, et al. (2002). "Silver coated materials for external fixation devices: in vitro biocompatibility and genotoxicity." Biomaterials **23**(3): 887-892.
- Bowen, B. and N. Epstein (1979). "Fine particle deposition in smooth parallel-plate channels." Journal of Colloid and Interface Science **72**(1): 81-97.
- Brant, J., H. Lecoanet, et al. (2005). "Aggregation and deposition characteristics of fullerene nanoparticles in aqueous systems." Journal of Nanoparticle Research **7**(4): 545-553.
- Bruck, S. (1972). "Biomaterials in medical devices." ASAIO Journal **18**(1): 1.
- Buddemeier, R. and J. Hunt (1988). "Transport of colloidal contaminants in groundwater: Radionuclide migration at the Nevada Test Site." Applied Geochemistry **3**(5): 535-548.
- Busscher, H., J. Sjollema, et al. (1990). "Relative importance of surface free energy as a measure of hydrophobicity in bacterial adhesion to solid surfaces."
- Casimir, H. and D. Polder (1946). "Influence of retardation on the london-van der waals forces." Nature **158**: 787-788.
- Chen, K. L. and M. Elimelech (2006). "Aggregation and deposition kinetics of fullerene (C-60) nanoparticles." Langmuir **22**(26): 10994-11001.
- Chen, K. L. and M. Elimelech (2008). "Interaction of Fullerene (C-60) Nanoparticles with Humic Acid and Alginate Coated Silica Surfaces: Measurements, Mechanisms, and Environmental Implications." Environmental Science & Technology **42**(20): 7607-7614.
- Chryssolouris, G., P. Stavropoulos, et al. (2004). "Nanomanufacturing processes: a critical review." International Journal of Materials and Product Technology **21**(4): 331-348.

- Clark, S., D. Lawler, et al. (1992). "Contact filtration: particle size and ripening." Journal American Water Works Association **84**(12): 61-71.
- Colvin, V. (2003). "The potential environmental impact of engineered nanomaterials." Nature biotechnology **21**(10): 1166-1170.
- Corapcioglu, M. and S. Jiang (1993). "Colloid-facilitated groundwater contaminant transport." Water Resources Research **29**(7).
- Cornell, R. and U. Schwertmann (1996). The iron oxides, VCH Weinheim.
- Creighton, J., C. Blatchford, et al. (1979). "Plasma resonance enhancement of Raman scattering by pyridine adsorbed on silver or gold sol particles of size comparable to the excitation wavelength." Journal of the Chemical Society, Faraday Transactions 2 **75**: 790-798.
- Czarnecki, J. (1986). "The effects of surface inhomogeneities on the interactions in colloidal systems and colloid stability." Advances in colloid and interface science **24**(4): 283-319.
- Czarnecki, J. and V. Itschenskij (1984). "Van der Waals attraction energy between unequal rough spherical particles." Journal of Colloid and Interface Science **98**(2): 590-591.
- Dahneke, B. (1974). "Diffusional deposition of particles." Journal of Colloid and Interface Science **48**(3): 520-522.
- Debye, P. (1929). Polar molecules, The Chemical Catalog Company, inc.
- Debye, P. and E. Huckel (1923). "De la theories des electrolytes. I. Abaissement du point de congelation et phenomenes associes." Physikalische Zeitschrift **24**(9): 185-206.
- Derjaguin, B. (1940). "On the repulsive forces between charged colloid particles and on the theory of slow coagulation and stability of lyophobic sols." Transactions of the Faraday Society **35**: 203-215.
- Derjaguin, B. V. and L. Landau (1941). "Theory of the stability of strongly charged lyophobic sols and of the adhesion of strongly charged particles in solutions of electrolytes." Acta Phys.-Chim. USSR.

- Domingos, R., N. Tufenkji, et al. (2009). "Aggregation of titanium dioxide nanoparticles: role of a fulvic acid." Environmental Science & Technology **43**(5): 1282.
- Dukhin, S. and J. Lyklema (1987). "Dynamics of colloid particle interaction." Langmuir **3**(1): 94-98.
- Elimelech, M., J. Y. Chen, et al. (2003). "Particle deposition onto solid surfaces with micropatterned charge heterogeneity: The "hydrodynamic bump" effect." Langmuir **19**(17): 6594-6597.
- Elimelech, M., M. Nagai, et al. (2000). "Relative insignificance of mineral grain zeta potential to colloid transport in geochemically heterogeneous porous media." Environmental Science & Technology **34**(11): 2143-2148.
- Elimelech, M. and C. R. Omelia (1990). "Effect of particle-size on collision efficiency in the deposition of brownian particles with electrostatic energy barriers." Langmuir **6**(6): 1153-1163.
- Elimelech, M. and C. R. Omelia (1990). "Kinetics of deposition of colloidal particles in porous media." Environmental Science & Technology **24**(10): 1528-1536.
- Elimelech, M., R. Williams, et al. (1998). Particle deposition and aggregation: Measurement, modelling and simulation, Butterworth-Heinemann.
- Espinasse, B., E. M. Hotze, et al. (2007). "Transport and retention of colloidal aggregates of C-60 in porous media: Effects of organic macromolecules, ionic composition, and preparation method." Environmental Science & Technology **41**: 7396-7402.
- Feitz, A., S. Joo, et al. (2005). "Oxidative transformation of contaminants using colloidal zero-valent iron." Colloids and Surfaces A: Physicochemical and Engineering Aspects **265**(1-3): 88-94.
- Fuchs, N. (1934). "Über die Stabilität und Aufladung der Aerosole." Z. Physik(89): 736-743.
- Girshick, S. (2008). "Aerosol processing for nanomanufacturing." Journal of Nanoparticle Research **10**(6): 935-945.

- Grasso*, D., K. Subramaniam, et al. (2002). "A review of non-DLVO interactions in environmental colloidal systems." Reviews in Environmental Science and Biotechnology **1**(1): 17-38.
- Gregory, J. (1970). "The calculation of Hamaker constants." Advances in colloid and interface science **2**(4): 396-417.
- Gregory, J. (1975). "Interaction of unequal double layers at constant charge." Journal of Colloid and Interface Science **51**(1): 44-51.
- Gregory, J. (1981). "Approximate expressions for retarded van der Waals interaction." Journal of Colloid and Interface Science **83**(1): 138-145.
- Gregory, J. and A. Wishart (1980). "Deposition of latex particles on alumina fibers." Colloids and Surfaces **1**(3-4): 313-334.
- Grolimund, D., M. Borkovec, et al. (1996). "Colloid-facilitated transport of strongly sorbing contaminants in natural porous media: a laboratory column study." Environ. Sci. Technol **30**(10): 3118-3123.
- Gurav, A., T. Kodas, et al. (1993). "Aerosol processing of materials." Aerosol science and technology **19**(4): 411-452.
- Guzman, K., M. Taylor, et al. (2006). "Environmental Risks of Nanotechnology: National Nanotechnology Initiative Funding, 2000- 2004." Environ. Sci. Technol **40**(5): 1401-1407.
- Hahn, M. W., D. Abadzic, et al. (2004). "Aguasols: On the role of secondary minima." Environmental Science & Technology **38**(22): 5915-5924.
- Hahn, M. W. and C. R. O'Melia (2004). "Deposition and reentrainment of Brownian particles in porous media under unfavorable chemical conditions: Some concepts and applications." Environmental Science & Technology **38**(1): 210-220.
- Hamaker, H. (1937). "The London--van der Waals attraction between spherical particles." physica **4**(10): 1058-1072.
- Hench, L. and J. West (1990). "The sol-gel process." Chemical Reviews **90**(1): 33-72.

- Hiemenz, P. and R. Rajagopalan (1997). Principles of colloid and surface chemistry, CRC.
- Ho, N. and W. Higuchi (1968). "Preferential aggregation and coalescence in heterodispersed systems." Journal of Pharmaceutical Sciences **57**(3): 436-442.
- Hoet, P., A. Nemmar, et al. (1999). "Health impact of nanomaterials?" Toxicol. Sci **52**: 209-216.
- Hogg, R., T. Healy, et al. (1966). "Mutual coagulation of colloidal dispersions." Transactions of the Faraday Society **62**: 1638-1651.
- Hsu, B., C. Huang, et al. (2001). "Filtration behaviors of Giardia and Cryptosporidium ionic strength and pH effects." Water Research **35**(16): 3777-3782.
- Hull, M. and J. Kitchener (1969). "Interaction of spherical colloidal particles with planar surfaces." Transactions of the Faraday Society **65**: 3093-3104.
- Hunter, R., L. White, et al. (1987). Foundations of colloid science, Clarendon Press Oxford.
- Israelachvili, J. (1992). Intermolecular and surface forces, Academic press London.
- Israelachvili, J. and P. McGuiggan (1988). "Forces between surfaces in liquids." Science **241**(4867): 795.
- Ives, K. and J. Gregory (1966). Surface forces in filtration.
- Jaisi, D., N. Saleh, et al. (2008). "Transport and filtration of carbon nanotubes in porous media." Geochimica et Cosmochimica Acta Supplement **72**: 422.
- Jaroniec, M. and R. Madey (1988). "Physical adsorption on heterogeneous solids." Studies in physical and theoretical chemistry **59**.
- Johnson, P. R., N. Sun, et al. (1996). "Colloid transport in geochemically heterogeneous porous media: Modeling and measurements." Environmental Science & Technology **30**(11): 3284-3293.

- Kanel, S., H. Choi, et al. (2007). "Transport characteristics of surface-modified nanoscale zero-valent iron in porous media." Water Science & Technology **55**(1-2): 157-162.
- Keesom, W. (1921). "Die van der waalsschen kohasionskrafte." Physikalische Zeit **22**: 129.
- Kessler, J. and J. Hunt "Dissolved and colloidal contaminant transport in a partially clogged fracture." Water Resources Research **30**(4).
- Kihira, H. and E. Matijevic (1992). "An assessment of heterocoagulation theories." Advances in colloid and interface science **42**: 1-31.
- Kodas, T. and M. Hampden-Smith (1999). Aerosol processing of materials, Vch Verlagsgesellschaft Mbh.
- Koopal, L., S. Dukhin, et al. (1993). "Modelling of the double layer and electrosorption of a patchwise heterogeneous surface on the basis of its homogeneous analogue. I: Non-interacting patches. Discussion." Colloids and surfaces. A, Physicochemical and engineering aspects **73**: 201-209.
- Koopal, L. and W. Van Riemsdijk (1989). "Electrosorption on random and patchwise heterogeneous surfaces: electrical double-layer effects." Journal of Colloid and Interface Science **128**(1): 188-200.
- Kosmulski, M. (2001). Chemical properties of material surfaces, CRC.
- Kuin, A. (1990). "Interaction potential of a dispersion of colloidal particles with a non-homogeneous surface potential." Faraday Discussions of the Chemical Society **90**: 235-244.
- Lahoussine-Turcaud, V. and M. Wiesner (1990). "Fouling in tangential-flow ultrafiltration. The effect of colloid size and coagulation pretreatment." Journal of membrane science **52**(2): 173-190.
- Lakshmi, B., C. Patrissi, et al. (1997). "Sol- Gel Template Synthesis of Semiconductor Oxide Micro-and Nanostructures." Chem. Mater **9**(11): 2544-2550.
- Lecoanet, H., J. Bottero, et al. (2004). "Laboratory assessment of the mobility of nanomaterials in porous media." Environ. Sci. Technol **38**(19): 5164-5169.

- Leeuwen, H. and J. Lyklema "Interfacial electrodynamics of interacting colloidal particles. Geometrical aspects."
- Levich, V. (1962). *Physicochemical Hydrodynamics.* , Prentice Hall, Englewood Cliffs, NJ.
- Lim, A. and R. Bai (2003). "Membrane fouling and cleaning in microfiltration of activated sludge wastewater." *Journal of membrane science* **216**(1-2): 279-290.
- Lin, S. and M. Wiesner (2010). "Exact Analytical Expressions for the Potential of Electrical Double Layer Interactions for a Sphere- Plate System." *Langmuir*: 2993-3009.
- Litton, G. and T. Olson (1993). "Colloid deposition rates on silica bed media and artifacts related to collector surface preparation methods." *Environmental Science & Technology* **27**(1): 185-193.
- Litton, G. and T. Olson (1996). "Particle size effects on colloid deposition kinetics: evidence of secondary minimum deposition." *Colloids and Surfaces A: Physicochemical and Engineering Aspects* **107**: 273-283.
- Liu, Y., S. Majetich, et al. (2005). "TCE dechlorination rates, pathways, and efficiency of nanoscale iron particles with different properties." *Environ. Sci. Technol* **39**(5): 1338-1345.
- Liu, Y., T. Phenrat, et al. (2007). "Effect of TCE concentration and dissolved groundwater solutes on NZVI-promoted TCE dechlorination and H₂ evolution." *Environ. Sci. Technol* **41**(22): 7881-7887.
- Logan, B., T. Hilbert, et al. (1993). "Removal of bacteria in laboratory filters: models and experiments." *Water Research* **27**(6): 955-962.
- London, F. (1930). "Theory and systematics of molecular forces." *Z. Phys* **63**: 245.
- Ludwig, P., G. Peschel, et al. (1988). "Evidence for secondary minimum coagulation in a silica hydrosol obtained by dynamic light scattering." *Dispersed systems*: 146.
- Lyklema, J., H. Van Leeuwen, et al. (2005). *Fundamentals of interface and colloid science*, Academic Pr.

- Mallevalle, J., P. Odendaal, et al. (1996). Water treatment membrane processes, McGraw-Hill Professional.
- Marshall, J. and J. Kitchener (1966). "The deposition of colloidal particles on smooth solids." J. Colloid Interface Sci **22**: 342.
- Martin, R., E. Bouwer, et al. (1992). "Application of clean-bed filtration theory to bacterial deposition in porous media." Environmental Science & Technology **26**(5): 1053-1058.
- McCarthy, J. and J. Zachara (1989). "Subsurface transport of contaminants." Environmental Science & Technology **23**(5): 496-502.
- McFarland, A. and R. Van Duyne (2003). "Single silver nanoparticles as real-time optical sensors with zeptomole sensitivity." Nano letters **3**(8): 1057-1062.
- Miklavic, S., D. Chan, et al. (1994). "Double layer forces between heterogeneous charged surfaces." The Journal of Physical Chemistry **98**(36): 9022-9032.
- Montgomery, J. (1985). "Water treatment principles and design." JOHN WILEY AND SONS, NEW YORK, NY(USA). 1985.
- Moran, D., M. Moran, et al. (1993). "Particle Behavior in Deep-Bed Filtration: Part 1- Ripening and Breakthrough." Journal American Water Works Association **85**(12): 69-81.
- Mylon, S., K. Chen, et al. (2004). "Influence of natural organic matter and ionic composition on the kinetics and structure of hematite colloid aggregation: Implications to iron depletion in estuaries." Langmuir **20**(21): 9000-9006.
- Nazemifard, N., J. Masliyah, et al. (2006). "Particle deposition onto micropatterned charge heterogeneous substrates: Trajectory analysis." Journal of Colloid and Interface Science **293**(1): 1-15.
- O'MELIA, C. and W. Stumm (1967). "Theory of water filtration."
- Overbeek, J. (1982). "Strong and weak points in the interpretation of colloid stability." Advances in Colloid and Interface Chemistry **16**: 1730.

- Panacek, A., L. Kvittek, et al. (2006). "Silver colloid nanoparticles: synthesis, characterization, and their antibacterial activity." J. Phys. Chem. B **110**(33): 16248-16253.
- Penners, N. and L. Koopal (1987). "The effect of particle size on the stability of haematite ([alpha]-Fe₂O₃) hydrosols." Colloids and Surfaces **28**: 67-83.
- Phenrat, T., N. Saleh, et al. (2008). "Stabilization of aqueous nanoscale zerovalent iron dispersions by anionic polyelectrolytes: adsorbed anionic polyelectrolyte layer properties and their effect on aggregation and sedimentation." Journal of Nanoparticle Research **10**(5): 795-814.
- Phenrat, T., N. Saleh, et al. (2007). "Aggregation and sedimentation of aqueous nanoscale zerovalent iron dispersions." Environ. Sci. Technol **41**(1): 284-290.
- Pieper, A., J. Ryan, et al. (1997). "Transport and recovery of bacteriophage PRD1 in a sand and gravel aquifer: Effect of sewage-derived organic matter." Environ. Sci. Technol **31**(4): 1163-1170.
- Prieve, D. and E. Ruckenstein (1980). "Role of surface chemistry in primary and secondary coagulation and heterocoagulation." Journal of Colloid and Interface Science **73**(2): 539-555.
- Puls, R. and R. Powell (1992). "Transport of inorganic colloids through natural aquifer material: Implications for contaminant transport." Environmental Science & Technology **26**(3): 614-621.
- Quevedo, I. and N. Tufenkji (2009). "Influence of solution chemistry on the deposition and detachment kinetics of a CdTe quantum dot examined using a Quartz crystal microbalance." Environmental Science & Technology **43**(9): 3176.
- Rajagopalan, R. and R. Chu (1982). "Dynamics of adsorption of colloidal particles in packed beds." Journal of Colloid and Interface Science **86**(2): 299-317.
- Rajagopalan, R. and C. Tien (1976). "Trajectory analysis of deep-bed filtration with the sphere-in-cell porous media model." AIChE Journal **22**(3): 523-533.
- Rebecca, A. and K. Bojeong (2009). "Influence of ionic strength, pH, and cation valence on aggregation kinetics of titanium dioxide nanoparticles." Environmental Science & Technology **43**(5).

- Redman, J., S. Walker, et al. (2004). "Bacterial adhesion and transport in porous media: Role of the secondary energy minimum." Environmental Science & Technology **38**(6): 1777-1785.
- Reerink, H. and J. Overbeek (1954). "The rate of coagulation as a measure of the stability of silver iodide sols." Discussions of the Faraday Society **18**: 74-84.
- Renn, O. and M. Roco (2006). "Nanotechnology and the need for risk governance." Journal of Nanoparticle Research **8**(2): 153-191.
- Richmond, P. (1974). "Electrical forces between particles with arbitrary fixed surface charge distributions in ionic solution." Journal of the Chemical Society, Faraday Transactions 2 **70**: 1066-1073.
- Richmond, P. (1975). "Electrical forces between particles with discrete periodic surface charge distributions in ionic solution." Journal of the Chemical Society, Faraday Transactions 2 **71**: 1154-1163.
- Robichaud, C., D. Tanzil, et al. (2005). "Relative risk analysis of several manufactured nanomaterials: An insurance industry context." Environmental Science & Technology **39**(22): 8985-8994.
- Ruckenstein, E. and D. Prieve (1976). "Adsorption and desorption of particles and their chromatographic separation." AIChE Journal **22**(2): 276-283.
- Ryan, J., M. Elimelech, et al. (1999). "Bacteriophage PRD1 and silica colloid transport and recovery in an iron oxide-coated sand aquifer." Environ. Sci. Technol **33**(1): 63-73.
- Ryan, J. and P. Gschwend (1992). "Effect of iron diagenesis on the transport of colloidal clay in an unconfined sand aquifer." Geochim. Cosmochim. Acta **56**: 1507-1521.
- Ryan, J. N. and M. Elimelech (1996). "Colloid mobilization and transport in groundwater." Colloids and Surfaces a-Physicochemical and Engineering Aspects **107**: 1-56.
- Ryde, N., H. Kihira, et al. (1992). "Particle adhesion in model systems. 15. Effect of colloid stability in multilayer deposition." J. Colloid Interface Sci **151**(2): 421-432.
- Saleh, N., T. Phenrat, et al. (2005). "Adsorbed triblock copolymers deliver reactive iron nanoparticles to the oil/water interface." Nano Lett **5**(12): 2489-2494.

- Schenkel, J. and J. Kitchener (1960). "A test of the Derjaguin-Verwey-Overbeek theory with a colloidal suspension." Transactions of the Faraday Society **56**: 161-173.
- Schumann, D. (1984). "Perturbations to the electrophoretic mobility due to electrical surface effects." PCH PhysicoChemical Hydrodynamics **5**(5): 383-388.
- Schumann, D. and B. D'EPENOUX (1987). "The effect of electrical nonhomogeneities of particles on mean surface potential." Journal of Colloid and Interface Science **116**(1): 159-167.
- Shiraishi, Y. and N. Toshima (1999). "Colloidal silver catalysts for oxidation of ethylene." Journal of Molecular Catalysis. A, Chemical **141**(1-3): 187-192.
- Silvert, P., R. Herrera-Urbina, et al. (1997). "Preparation of colloidal silver dispersions by the polyol process." Journal of Materials Chemistry **7**(2): 293-299.
- Sjollema, J., H. Busscher, et al. (1989). "Real-time enumeration of adhering microorganisms in a parallel plate flow cell using automated image analysis." Journal of Microbiological Methods **9**(2): 73-78.
- Song, L., P. Johnson, et al. (1994). "Kinetics of colloid deposition onto heterogeneously charged surfaces in porous media." Environmental Science & Technology **28**(6): 1164-1171.
- Song, L. F. and M. Elimelech (1994). "Transient deposition of colloidal particles in heterogeneous porous-media." Journal of Colloid and Interface Science **167**(2): 301-313.
- Song, L. F., P. R. Johnson, et al. (1994). "Kinetics of colloid deposition onto heterogeneously charged surfaces in porous media". Environmental Science & Technology **28**(6): 1164-1171.
- Spielman, L. and J. Fitzpatrick (1973). "Theory for particle collection under London and gravity forces." Journal of Colloid and Interface Science **42**(3): 607-623.
- Spielman, L. and S. Friedlander (1974). "Role of the electrical double layer in particle deposition by convective diffusion." Journal of Colloid and Interface Science **46**(1): 22-31.
- Sposito, G. (2008). The chemistry of soils, Oxford University Press, USA.

- Stumm, W., J. Morgan, et al. (1996). Aquatic chemistry, Wiley New York.
- Stumm, W., L. Sigg, et al. (1992). Chemistry of the solid-water interface, Wiley New York.
- Tien, C. and B. Ramarao (2007). Granular filtration of aerosols and hydrosols, Elsevier Science Ltd.
- Tobiason, J. (1987). "Physicochemical aspects of particle deposition in porous media." Geography and Environmental Engineering.
- Tobiason, J. and C. O'melia (1988). "Physicochemical aspects of particle removal in depth filtration." Journal American Water Works Association **80**(12): 54-64.
- Tratnyek, P. and R. Johnson (2006). "Nanotechnologies for environmental cleanup." Nano Today **1**(2): 44-48.
- Tufenkji, N. and M. Elimelech (1999). "Deviation from the classical colloid filtration theory in the presence of repulsive DLVO interactions." Water Resour. Res **35**(1797): 1807.
- Tufenkji, N. and M. Elimelech (2004). "Correlation equation for predicting single-collector efficiency in physicochemical filtration in saturated porous media." Environmental Science & Technology **38**(2): 529-536.
- Tufenkji, N. and M. Elimelech (2005). "Breakdown of colloid filtration theory: Role of the secondary energy minimum and surface charge heterogeneities." Langmuir **21**(3): 841-852.
- Vaidyanathan, R. and C. Tien (1991). "Hydrosol deposition in granular media under unfavorable surface conditions." Chemical Engineering Science **46**(4): 967-983.
- Veerapaneni, S. and M. Wiesner (1997). "Deposit morphology and head loss development in porous media." Environ. Sci. Technol **31**(10): 2738-2744.
- Verwey, E. (1935). "The Electrical Double Layer and the Stability of Lyophobic Colloids." Chemical Reviews **16**(3): 363-415.
- Verwey, E. and J. Overbeek (1948). Theory of the stability of lyophobic colloids, Elsevier, Amsterdam.

- Walker, S., J. Hill, et al. (2005). "Influence of growth phase on adhesion kinetics of *Escherichia coli* D21g." Applied and Environmental Microbiology **71**(6): 3093.
- Wang, H., G. White, et al. (1993). "Ferrihydrite, lepidocrocite, and goethite in coatings from east Texas vertic soils." Soil Science Society of America Journal **57**(5): 1381.
- Wiese, G. and T. Healy (1970). "Effect of particle size on colloid stability." Transactions of the Faraday Society **66**: 490-499.
- Wiesner, M. and J. Bottero (2007). Environmental nanotechnology: applications and impacts of nanomaterials, McGraw-Hill Professional.
- Wiesner, M. and J. Mallevialle (1989). "Membrane filtration of coagulated suspensions." Journal of Environmental Engineering **115**: 20.
- Wiesner, M. R., G. V. Lowry, et al. (2006). "Assessing the risks of manufactured nanomaterials." Environmental Science & Technology **40**(14): 4336-4345.
- Yao, K., M. Habibian, et al. (1971). "Water and waste water filtration. Concepts and applications." Environmental Science & Technology **5**(11): 1105-1112.
- Yao, K. M. and C. R. O'Melia (1968). "Particle Transport in Aqueous Flow Through Porous Media." Annual Conference of the Hydraulic Division of ASCE.
- Yoshimura, Y. (1980). "Initial particle collection mechanism in clean, deep-bed filtration." D. Eng. Dissertation, Kyoto University.
- Zhang, S. (2003). "Fabrication of novel biomaterials through molecular self-assembly." Nature biotechnology **21**(10): 1171-1178.